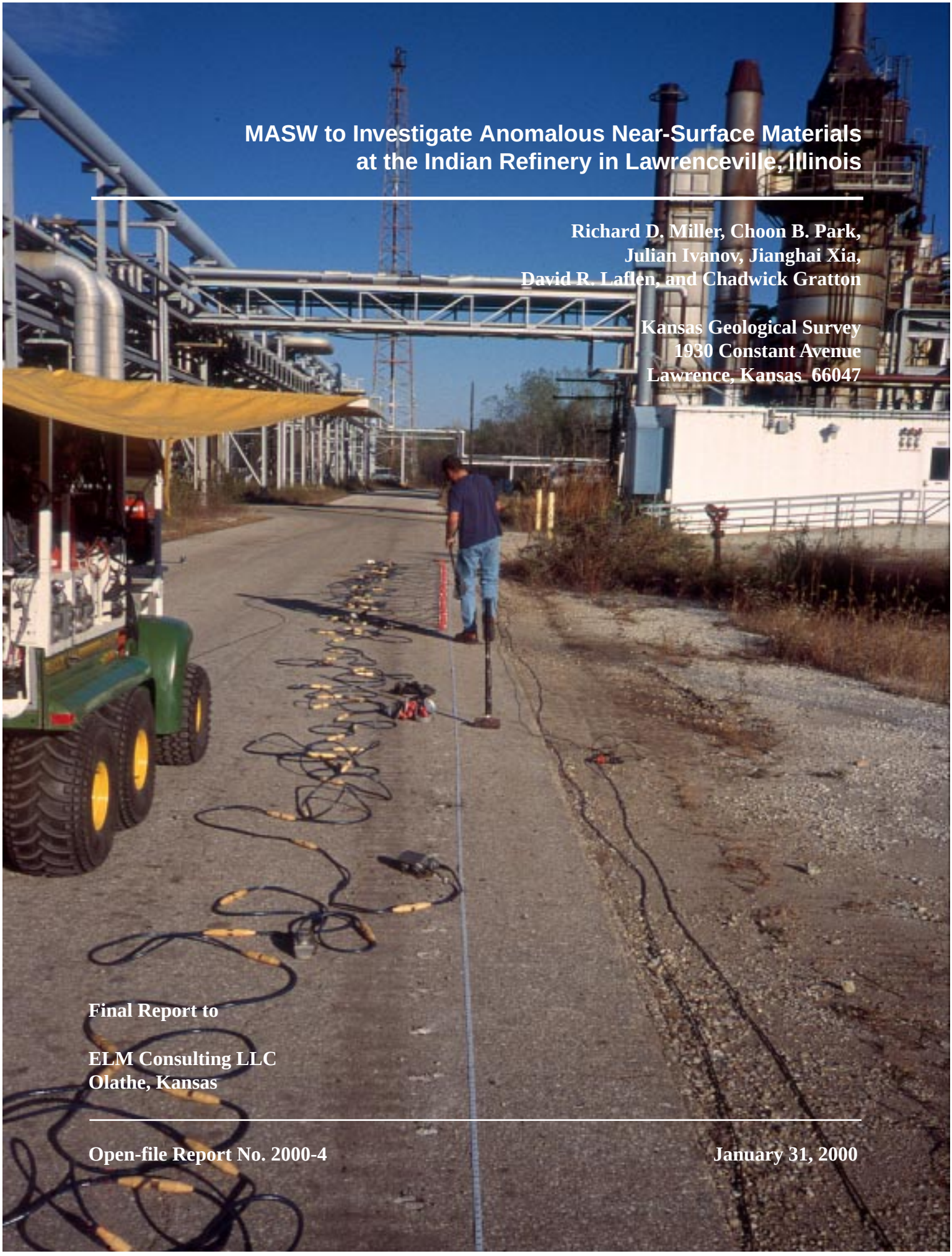

MASW to Investigate Anomalous Near-Surface Materials at the Indian Refinery in Lawrenceville, Illinois

Richard D. Miller, Choon B. Park, Julian Ivanov, Jianghai Xia, David R. Laflen, and Chadwick Gratton

Kansas Geological Survey
1930 Constant Avenue
Lawrence, Kansas 66047

Final Report to

ELM Consulting LLC
Olathe, Kansas

Open-file Report No. 2000-4

January 31, 2000

MASW to Investigate Anomalous Near-Surface Materials at the Indian Refinery in Lawrenceville, Illinois

by

Richard D. Miller
Choon B. Park
Julian M. Ivanov
Jianghai Xia
David R. Laflen
Chadwick Gratton

of the

Kansas Geological Survey
1930 Constant Avenue
Lawrence, KS 66047-3726

Final Report to

Randy Overton
ELM Consulting LLC
304 South Clairborne, Suite 200
Olathe, KS 66062

Open-file Report No. 2000-4

January 31, 2000

MASW to Investigate Anomalous Near-Surface Materials at the Indian Refinery in Lawrenceville, Illinois

Summary

The shear wave velocity field, calculated using the Multi-channel Analysis of Surface Waves (MASW) method (Park et al., 1999; Xia et al., 1999), and disturbances observed in the groundroll wavetrain transformations (phase and amplitude) were used to help identify variability in the lateral continuity of near-surface layers beneath asphalt roads within the Lawrenceville Refinery, settling ponds in and around the refinery property, surface remediated burial pits, and containment berms (Figure 1). Depths of investigation extended from a few feet below ground surface (BGS) to as much as 100 ft BGS on line 5. Anomalies interpreted within the soft sediments along all five lines are related to lateral changes in material properties. Confirmation and/or enhancement of interpretations of these data will require subsurface sampling. When comparing results from this study to previous investigations using this surface wave imaging technology at sites around the country (Miller and Xia, 1999a; Miller and Xia, 1999b; Miller et al., 1999), it is interesting to note that in most cases interpreted zones of anomalous material possess a unique velocity pattern somewhat universally consistent with all features of the same kind (subsidence, fractures, bedrock, etc.). In most cases, low velocity closures within the shear wave velocity field are indicative of "anomalies." Each profile collected in association with this feasibility test at the Lawrenceville Refinery was designed with a specific imaging objective in mind. The success of each profile can only be determined by a drilling program specifically designed to evaluate these findings.

Calculating the shear wave velocity field from surface wave arrivals can generally be accomplished with a high degree of accuracy regardless of cultural noise or obstacles. Data for this study were acquired in and around areas with occupied personal residences, railroad noise, site demolition activities, and normal industrial background noise (60 Hz, running motors, vehicle activity, etc.). A wide range of surface conditions required adaptations be made to optimize source and receiver coupling to cement and asphalt. Care was taken to insure no data carried artifacts related to surface features or background noise and that all data were acquired with special attention placed on the spread location relative to surface materials and structures. Comparisons of data characteristics recorded from geophones with steel baseplates to those with spikes revealed no significant difference in wavetrain properties or calculated dispersion curves.

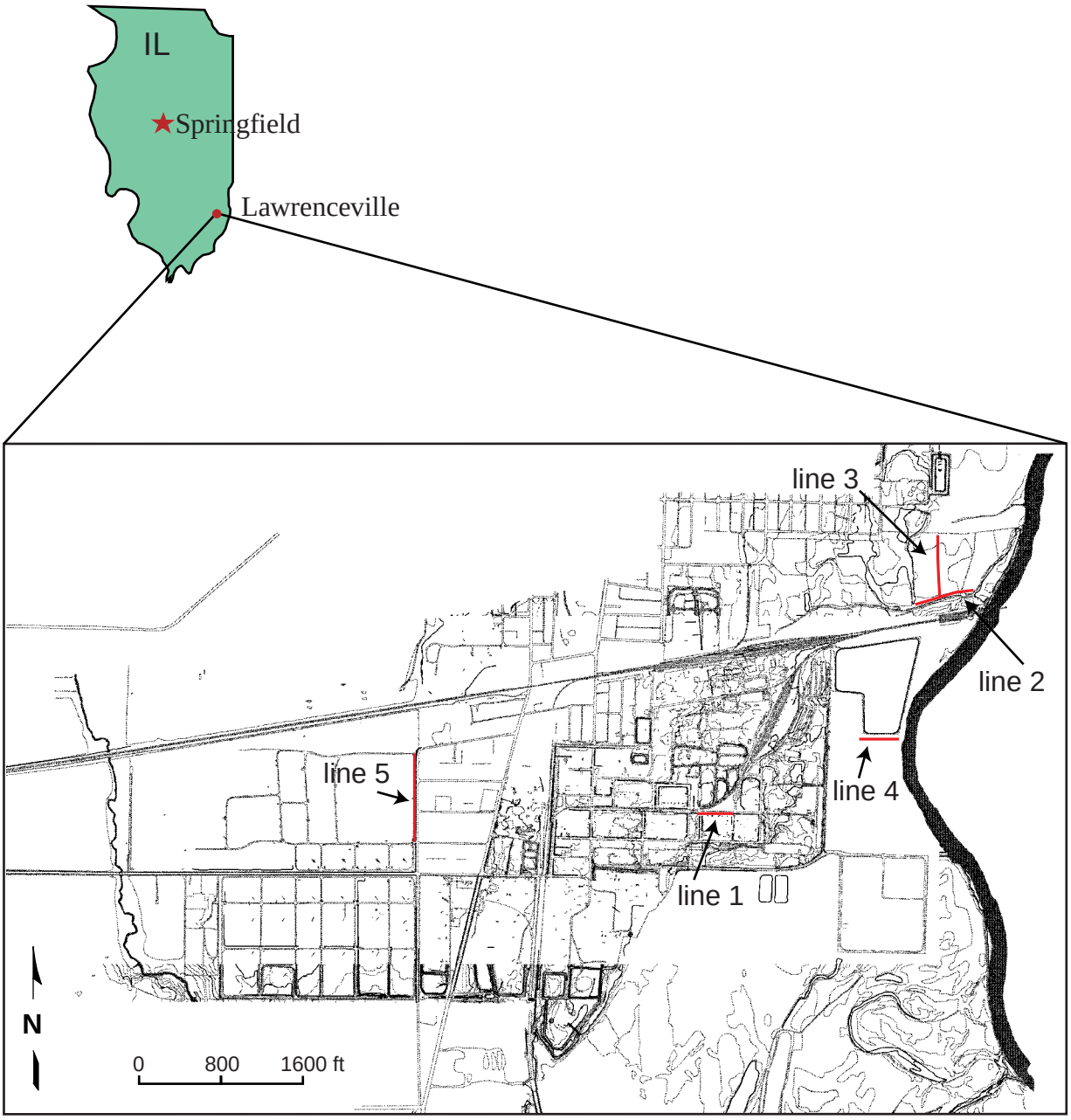

Figure 1. Site map and location of seismic lines.

Unlike recording concerns prominent when using other types of acoustic waves, surface waves seem to have only limited dependence on changes in receiver coupling. Non-source noise recorded on surface wave data reduces the quality of the dispersion curve but does not usually prevent an accurate and robust inversion.

MASW provides shear wave velocity profiles that accurately (15%) represent average shear wave velocities for a particular subsurface volume (Xia et al., 2000). Velocities measured during this study ranged from just over 200 ft/sec to around 2500 ft/sec. Localized changes of over 700 ft/sec (300%) across distances less than 10 ft were common around areas with observed structural damage. Velocity inversions laterally consistent over significant distances are evident within the upper 10 ft along most lines and likely relate to stiffer clays or partially cemented sediments in close proximity to sand or gravel zones. The sensitivity of shear wave velocities to changes in sediment makeup within this alluvial setting allowed even subtle changes in near-surface material properties to be identified on 2-D cross-sections. Uniquely locating localized zones of anomalous subsurface sediments (fill, sludge, or rubble) and/or objects (such as pipes, trenches, or old landfill materials) was possible with data from lines 1, 2, 3, and 4. Localized zones of lower velocity material can easily be picked out on lines 1 and 4. Line 3 provides a glimpse at an erosional surface beneath the base of the lower velocity fill materials. It takes very little imagination to interpret the well-defined low velocity zones extending down to depths of almost 10 ft at burial pits interpreted along line 4. Line 5 presents a reasonable depiction of the dike and relatively coherent sediments from the base of the dike down to about 100 ft BGS. Bedrock or a significant increase in velocity is evident at depth on lines 1, 2, 3, and 5. Each type of target imaged during this survey possesses a unique signature with each of the different imaging methods used. Interpreting these data requires incorporation of drilling, borehole measurements, and other geophysical soundings.

Interpreting changes in lithology with this technique has routinely involved correlating high velocity gradients and measured velocities to ground truth. Velocity fields along these five profiles possess relatively uniform increases in shear wave velocity from the surface to the maximum depth of the survey. Anomalous (relative to surrounding materials) high and low velocity closures, likely indicative of extreme lateral variability in material properties or foreign materials, are evident within the unconsolidated sediments along most of the lines. Several localized changes in shear wave velocity are strong candidates for drill investigation. Coherent

layers (bedding, changes in lithology, structural features, etc.) were interpreted based on velocity gradients, consistent changes in velocity contours, and overall velocity trends. Several possible explanations exist for each of these velocity phenomena. With the inherent nonuniqueness of these data, precisely located borings would be necessary along each of these lines to increase the confidence and/or modify these interpretations.

Large velocity gradients in the shear wave velocity field are likely indicative of changes in lithology (i.e., alluvial/glacial contacts, alluvial/bedrock, glacial/bedrock), while localized lateral changes (contour closures) in the shear wave velocity within the unconsolidated section were considered evidence of infilling or altered native earth. Mapping the surface of lithologic contacts using shear wave velocity data combined with drill data will result in a significantly higher resolution subsurface map than grid style drilling alone at this site. Advantages of mapping variations in the shallow stratigraphy with the shear wave velocity field calculated from surface waves using MASW include sensitivity to velocity inversions, ease of generating and propagating surface wave energy in comparison to body wave energy, being oblivious to cultural noise (mechanical or electrical), and sensitivity to lateral changes in velocity.

Introduction

Surface waves traditionally have been viewed as noise on multichannel seismic data designed to image environmental, engineering, and groundwater targets (Steeples and Miller, 1990). A recent development incorporating concepts from spectral analysis of surface waves (SASW) developed for civil engineering applications (Nazarian et al., 1983) with multi-trace seismic acquisition methods commonly used for petroleum applications (Glover, 1959) shows great potential for detecting, and in some cases delineating, anomalous subsurface materials. Extending the common use of surface wave analysis techniques from estimating 1-D shear wave velocities to detection and/or imaging required a multichannel approach to data acquisition and processing. Integrating the MASW method with a CMP-style data acquisition permits the generation of a laterally continuous 2-D shear wave velocity field cross-section (Park et al., 1996; Xia et al., 1997; Xia et al., 1998; Park et al., 1999; Xia et al., 1999). The MASW method as used here requires minimal processing and is relatively insensitive to cultural interference. Mating MASW with the redundant sampling approach used in CMP data acquisition provides a non-

invasive method of delineating horizontal and vertical variations in near-surface material properties.

Continuous acquisition of multichannel surface wave data along linear transects has recently shown great promise in detecting shallow voids and tunnels (Park et al., 1998), mapping the bedrock surface (Xia et al., 1998; Miller and Xia, 1999a), locating remnants of underground mines (Park et al., 1999), and delineating fracture systems (Park et al., 1997; Miller and Xia, 1999b). Extending this technology from sporadic sampling to continuous imaging required the incorporation of MASW with concepts from the CDP method (Mayne, 1962). Integrating these two methodologies resulted in the generation of a laterally continuous 2-D cross-section of the shear wave velocity field. Cross-sections generated in this fashion contain specific information about the horizontal and vertical continuity and physical properties of materials as shallow as a few inches to over 300 ft BGS in some settings.

Areas with pits, trenches, or underground utilities are likely targets for this type of imaging. Decreases in the shear wave velocity related to reduced soil compaction or localized increases in shear wave velocity associated with compacted caps overlying buried trenches or pits dramatically affect the dispersive character of surface wave energy. Key to exploiting surface waves as a site characterization tool is their sensitivity to shear wave velocity, compressional wave velocity, density, and layering in the half space.

Several key characteristics of surface waves and surface wave imaging make application of this technique possible in areas and at sites where other geophysical tools have failed or provided inadequate results. First and probably foremost is the ease with which surface waves can be generated. The relative high amplitude nature of surface waves (in comparison to body waves) makes possible their application in areas with elevated levels of mechanic/acoustic noise. A layer over half space is all that is necessary to propagate surface waves. It is one of the few acoustic methods that does not require velocity to increase with depth and/or a contrast (i.e., velocity, density, or combination [acoustic impedance]). Conductivity of soils, electrical noise, conductive structures, and buried utilities all represent significant problems or at least important considerations for electrical or EM methods. These have little or no impact on the generation or propagation and generally have no influence on the processing or interpretation of surface wave data. This flexibility in acquisition and insensitivity to environmental noise allows successful use of shear wave velocity profiling in areas where other geophysical methods might be limited.

This study focused on acquiring data in several areas with distinctly different targets and near-surface conditions. It is the intent of these data to provide a sampling of the shear wave velocity field (directly related to stiffness), permitting anomalous zones thought to be pits, trenches, or underground utilities to be identified and to investigate the potential of this technique to map lithologic boundaries. It was our goal to identify characteristics unique to the various targets suspected to be present in the subsurface at each site in such a way as to allow identification of similar anomalous features at other sites where their location is not nearly as well known. Lines were deployed after considering the optimum sampling of subsiding materials, depth of interest, and type of target. For three of the five profiles, acquisition parameters were designed to target materials at depths between about 5 ft and 30 ft. Of the remaining two profiles, one focused on the 0 to 15 ft BGS depth range and the other was designed to sample materials between about 10 and 100 ft BGS. The primary objective of this study was to evaluate the effectiveness of the method to locate, identify, and delineate unique subsurface targets at each of these five uniquely different sites with sufficient resolution to allow drill confirmation.

Data Acquisition

Data were acquired so as to center the profile as close as possible to the proposed targets while optimizing subsurface sampling, energy propagation, and coupling. Standard CMP roll-along techniques were used to record nominal 48-channel shot records along each line. Asphalt and concrete surfaces necessitated the outfitting of geophones with metal baseplates. Geophones planted in grassy areas employed traditional 3" steel spikes and provide good coupling. A 60-channel Geometrics StrataView seismograph recorded several vertically stacked impacts from either an 8 lb hammer, a 20 lb hammer, or a 150 lb accelerated weight drop at each shot station. Single 4.5 Hz Geospace GS-11D geophones spaced 1 ft, 2 ft, or 4 ft apart (depending on the target depth) along each profile line optimally responded to frequencies from 5 Hz to 60 Hz. The source-to-nearest-receiver offset was nominally 2 ft, 12 ft, or 24 ft and source-to-farthest-receiver offset ranged from around 50 to over 120 ft, again depending on target depth. These various recording geometries and frequency ranges resulted in spread and data characteristics optimum for examining earth materials between about 2 and 100 ft of depth, depending on the site.

Data Processing

Each 48-trace shot gather was recorded with live receivers within the optimum recording window. Multichannel records were analyzed with *SurfSeis* (a proprietary software package of the Kansas Geological Survey), facilitating the use of MASW with continuous profiling techniques. Each shot gather generated one dispersion curve. Care was taken to insure the spectral properties of the t-x data (shot gathers) were consistent with the maximum and minimum f-v_c values (v_c is phase velocities of surface waves) contained in the dispersion curve. Each dispersion curve was individually inverted into an x-v_s trace. Gathering all x-v_s traces into shot station sequence order results in a 2-D grid of the shear wave velocity field. The shear wave velocity field generated in this fashion does "smear" to a limited extent gradational velocity anomalies and requires an understanding of the overall resolution. The processing flow generally included the following steps:

SEG-2 to KGS-modified SEG-Y
Calculate the dispersion curve from phase velocity as function of frequency
Estimate initial model (5 Hz to 35 Hz—15 to 250 ft wavelength)
Invert to solve for shear wave velocity
Contour velocity field (*SURFER*®)

Data from all five lines were also processed to enhance disturbances in the surface wave energy field. Examining disturbances in the wavefield was made possible through processing the data through a wavefield transformation of common offset gathers of individual traces as well as using pattern recognition techniques with data that has been linearly moved out to compensate for offset and traces stacked (Park et al., 1998). Traces are displayed in a fashion designed to be sensitive to disruptions in the wavefield at specific frequencies, which in turn can be correlated to depth using the empirical axiom _ wavelength = depth. The processing steps were as follows:

SEG-2 to KGS-modified SEG-Y
Transform from time to frequency domain
Linear moveout
Stack
Display *as* wiggle trace sections

Interpretation

The 2-D shear wave velocity cross-sections have several striking characteristics likely influenced by changes in lithology or material properties. Changes in material composition,

cementation, or compaction are likely related to rapid changes in the velocity gradient. Rapid changes in the velocity gradient and velocity values correlate quite well to lithologic and material changes inferred from historical records of this refinery site.

SITE 1—Inside refinery with shallow pipe targets

Seismic data for site 1 were collected along a single profile centered on a set of steel pipes that appear to pass directly beneath an asphalt access road (Figure 1). The line was acquired completely on the asphalt road using plates on geophones and an 8 lb hammer directly impacting the road surface. The geophone spacing was 1 ft with a 4 ft source offset. It is not known if more than the single set of pipes pass directly beneath the survey line, but it is clear that the potential does exist for multiple utility bundles to be present directly beneath the profile transect. Overhead piping, pumping stations, as well as sundry other refinery-related components were present all along the profile line.

Data possessed a usable bandwidth of 5 Hz to 100 Hz, equating to a minimum and maximum depth of penetration around 5 ft to 100 ft, respectively. Accuracy of inverted S-wave velocities has been estimated to be about 15%, therefore changes in velocity of about 100 ft/sec or more are significantly above the average error and relate to variability in geology. Since the contour interval was selected at 50 ft/sec, anomalies with closure on two or more contour lines are related to measurable changes in subsurface properties. Localized closures defined by a single contour may be related to geology, but for the level of certainty required on this study single contour closures are considered background and used only in establishing velocity trends. Velocity trends from line 1 are laterally consistent and gradationally increase in depth from east to west across the profile. This uniform dip of shallow layers to the east is likely related to the current position of the river just off the east end of this line.

Two distinct anomalies are evident on line 1 around stations 1100 and 1110 on the shear wave contoured sections (Figure 2). These features are over 50 ft west of the projection of the pipes (target of this survey) under the profile. These two anomalies have a signature that extends from about 2 ft to depths of nearly 10 ft BGS. Based on characteristics alone, it appears these high velocity anomalies are indicative of a trench or some kind of buried object not native to this area. Dispersion curves from line 1 are relatively consistent from shot gather to shot gather and possess a somewhat unique shape when in proximity of the anomalies around 1100 (Figure 3).

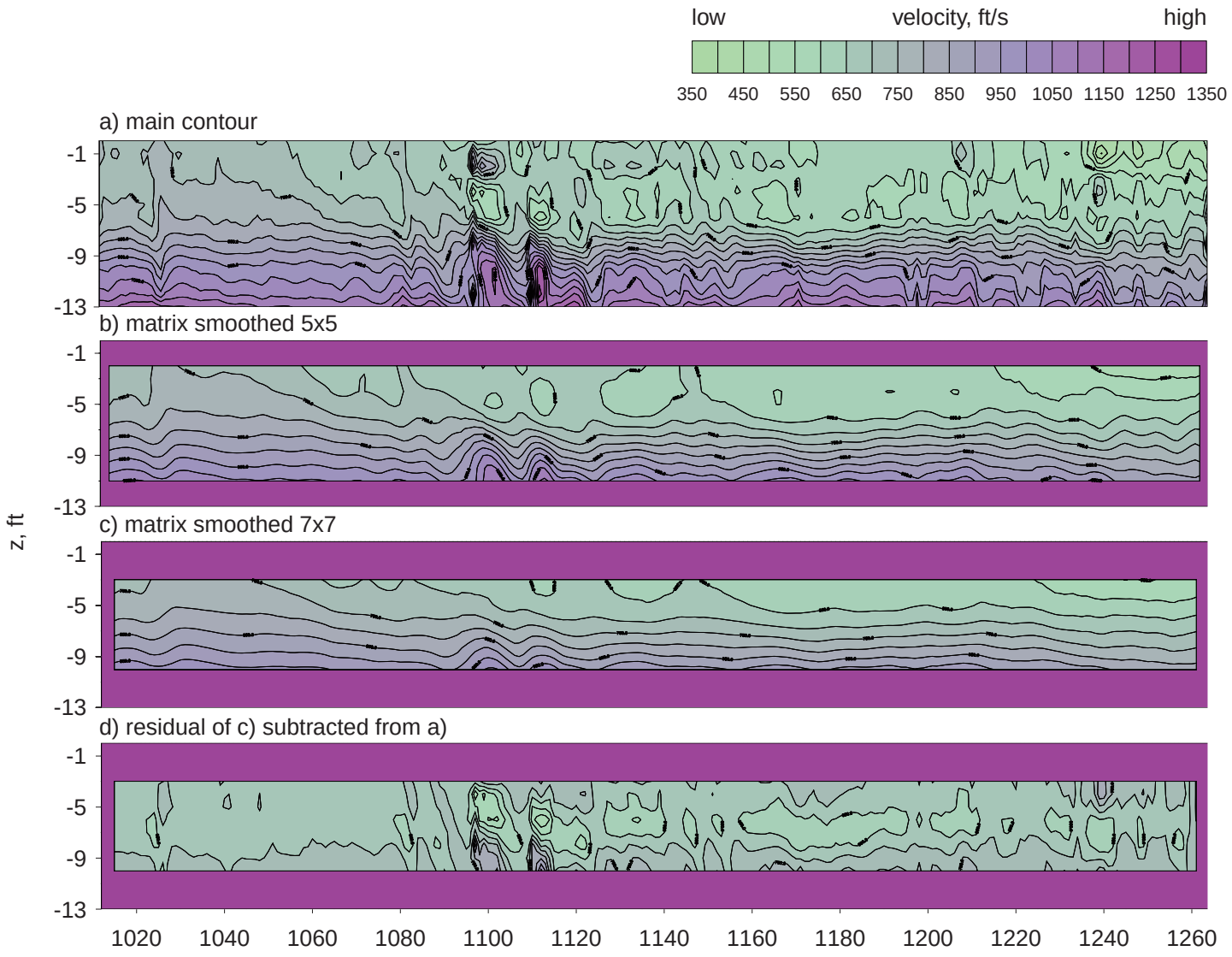

Figure 2A. (a) Shear wave velocity contour map of line 1 (b, c) with different degrees of smoothing applied and (d) residual.

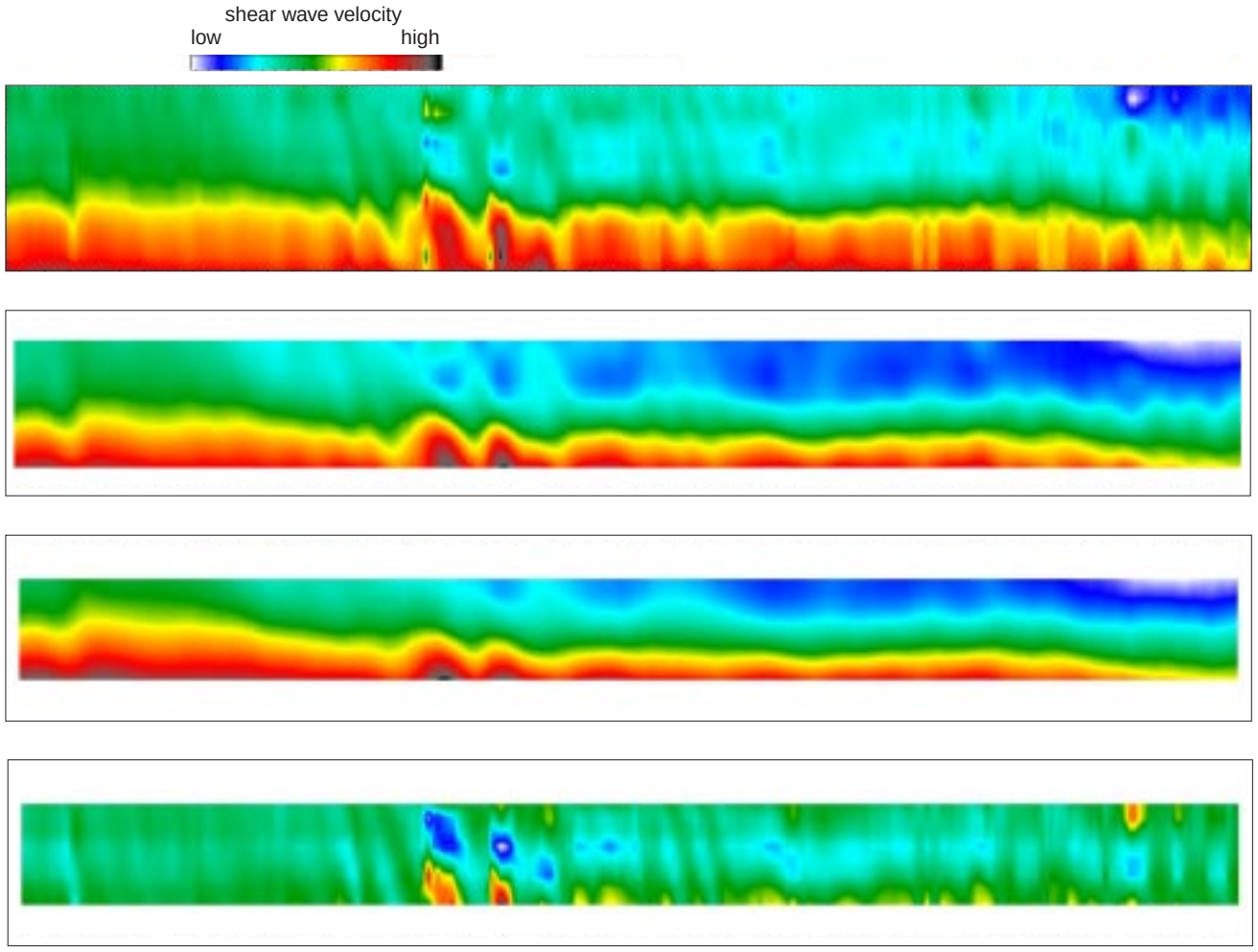

Figure 2B. Shear wave velocity contour color images of line 1 (data from Figure 2A).

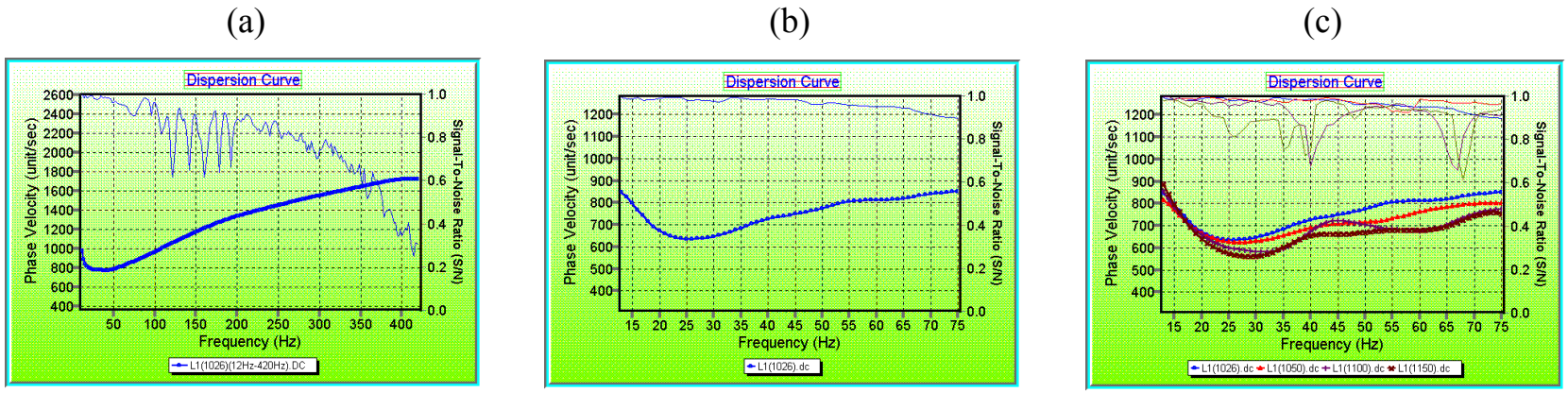

Figure 3. (a) Dispersion and signal-to-noise ratio (S/N) curve in the 12-420 Hz range for the second field record obtained along line 1. (b) Enlarged display of (a). (c) Dispersion and S/N curves for selected field records. Field records selected were evenly spaced along the line.

Signal-to-noise ratio, as evidenced by the thin line trace above the dispersion curve, suggests these data are dominated by ground roll. Observed breaks in the wavefield transformation at stations 1080, 1120, 1156, and 1230 are the direct result of abrupt changes in the subsurface material properties (Figure 4).

Comparison of common offset sections reveals a strong offset-dependent surface wave reflection that appears to be emanating from near-point source objects (Figures 5 and 6). At 8 ft source-to-receiver offset a strong diffraction-type pattern exists with an apex near station 1085. This is likely the same feature responsible for the low velocity anomalies evident on shear wave contours of line 1 (Figure 2). This correlation between two uniquely different processing methods and data attributes is strong evidence supporting investigation of this anomaly by a shallow borehole. After filtering, the 8 ft common offset section provides even stronger evidence in support of a prominent anomaly beneath station 1080 (Figure 7). Using a high frequency bandpass filter with only short offset traces, anomalies present in the shallowest part of the section become evident (Figure 8). Without a doubt, the west end of the profile possesses the strongest point-source type anomalies while still retaining areas that seem to be relatively undisturbed. On the other hand, the east end of the profile does not have as many pronounced point-source type anomalies, but it does have a significantly disturbed near-surface in general across the entire profile. From samples of shot gathers collected along the profile it is clear that the general shape of the dispersion curve remains relatively consistent, but each does have a subtle unique characteristics difference (Figure 9).

SITE 2—Outside fence immediately south of the tar pits

Seismic data for site 2 were collected along a single profile centered on the berm that separates the two tar pits and is immediately north of the access road paralleling the railroad tracks (Figure 1). The line was acquired completely on grass or dirt, permitting use of traditional spikes for the entire line. The source was a track vehicle-mounted accelerated weight drop. The geophone spacing was 4 ft with a 56 ft source-to-nearest-receiver offset. The subsurface structure is not well defined beneath this profile; it was the intent of this line to determine what could be resolved at depths of 30+ ft in this heavily filled area, undoubtedly dominated by alluvial deposition. It is possible that the fill placed during construction of the pits is very uniform and possesses no dramatic changes in compaction that would manifest themselves as anomalies on

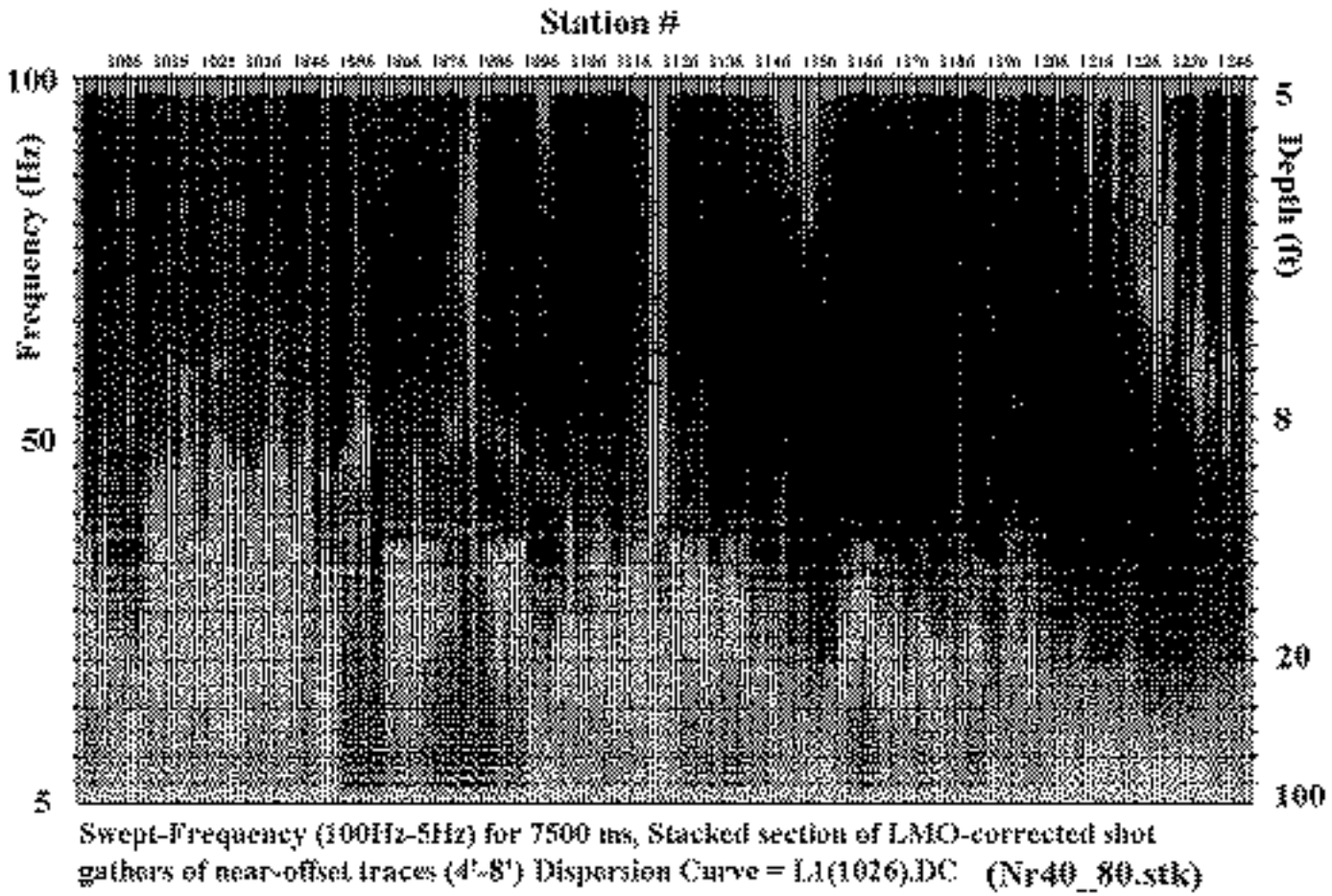

Figure 4. Wavefield transformation from line 1 of surface waves in 5-100 Hz range. Only near-offset traces (4, 5, 6, 7, 8 ft offsets) were selected in each shot gather, decomposed into swept-frequency format in 100-5 Hz range, linear-move-out (LMO) corrected using the phase velocity information in Figure 3(a), and then the five traces in each shot gather were stacked together to produce one stacked trace. Displayed image shows the collection of these stacked traces. The station number marked at top indicates the shot station number. On left-hand side of display is shown approximate frequency of the decomposed wavefield, and the approximate depth shown on right-hand side is calculated using the "half-wavelength" criterion. "Dark" parts in the section indicate that the elastic properties (velocities and attenuation properties) of the corresponding part of the near surface are the same as those below a surface location near the second shot station, and "white" parts indicate the opposite conditions.

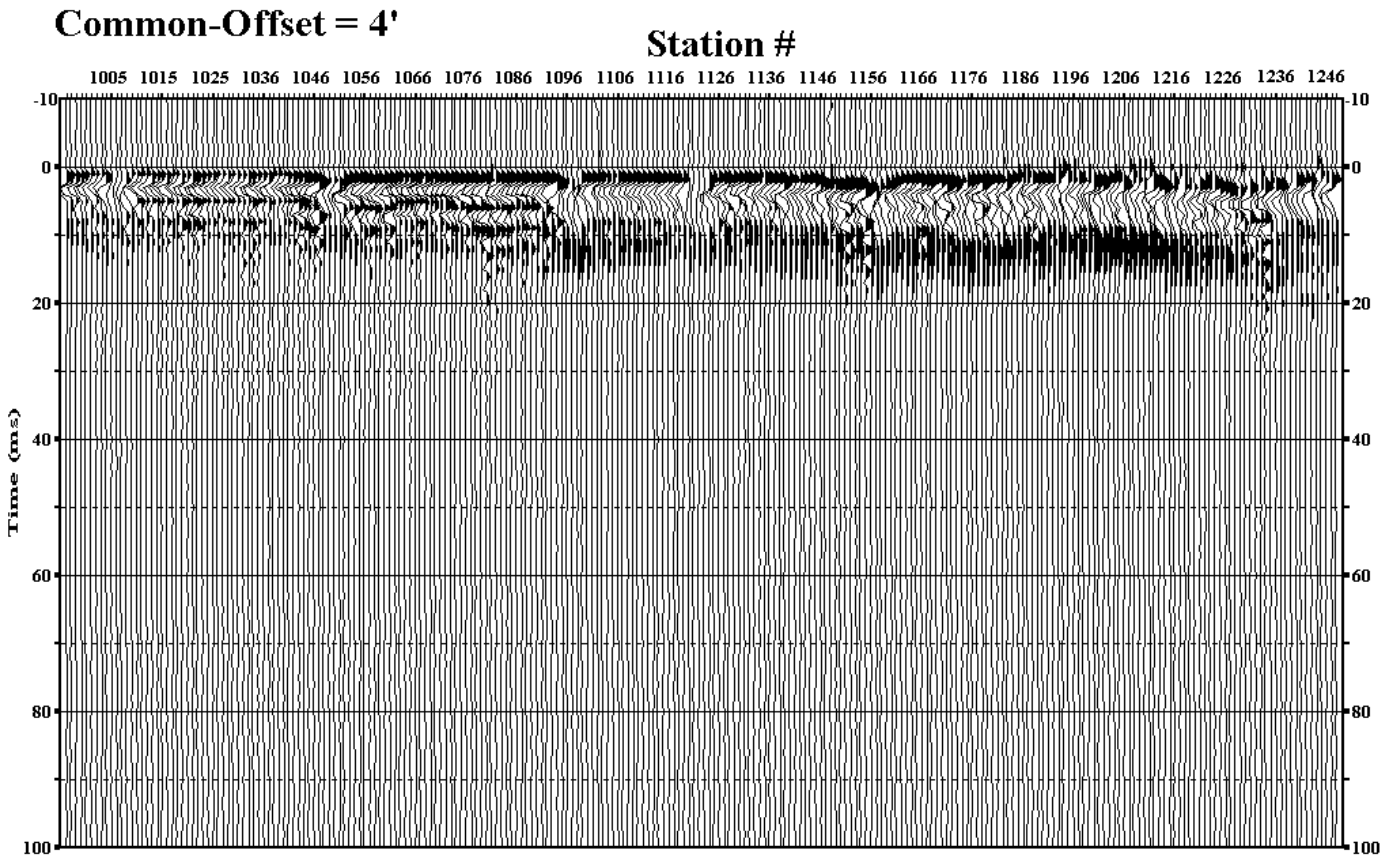

Figure 5. Common-offset (4 ft) section of field records from line 1. This section reveals a regional variation trend of near-surface elastic properties. Lack of a high-frequency component, for example, can be associated with possible existence of highly attenuative materials at shallow depths, and the discontinuities and hyperbolic moveouts of wavefields observed in both first arrivals and surface-waves can be associated with possible existence of near-surface anomalies (such as voids or pipes).

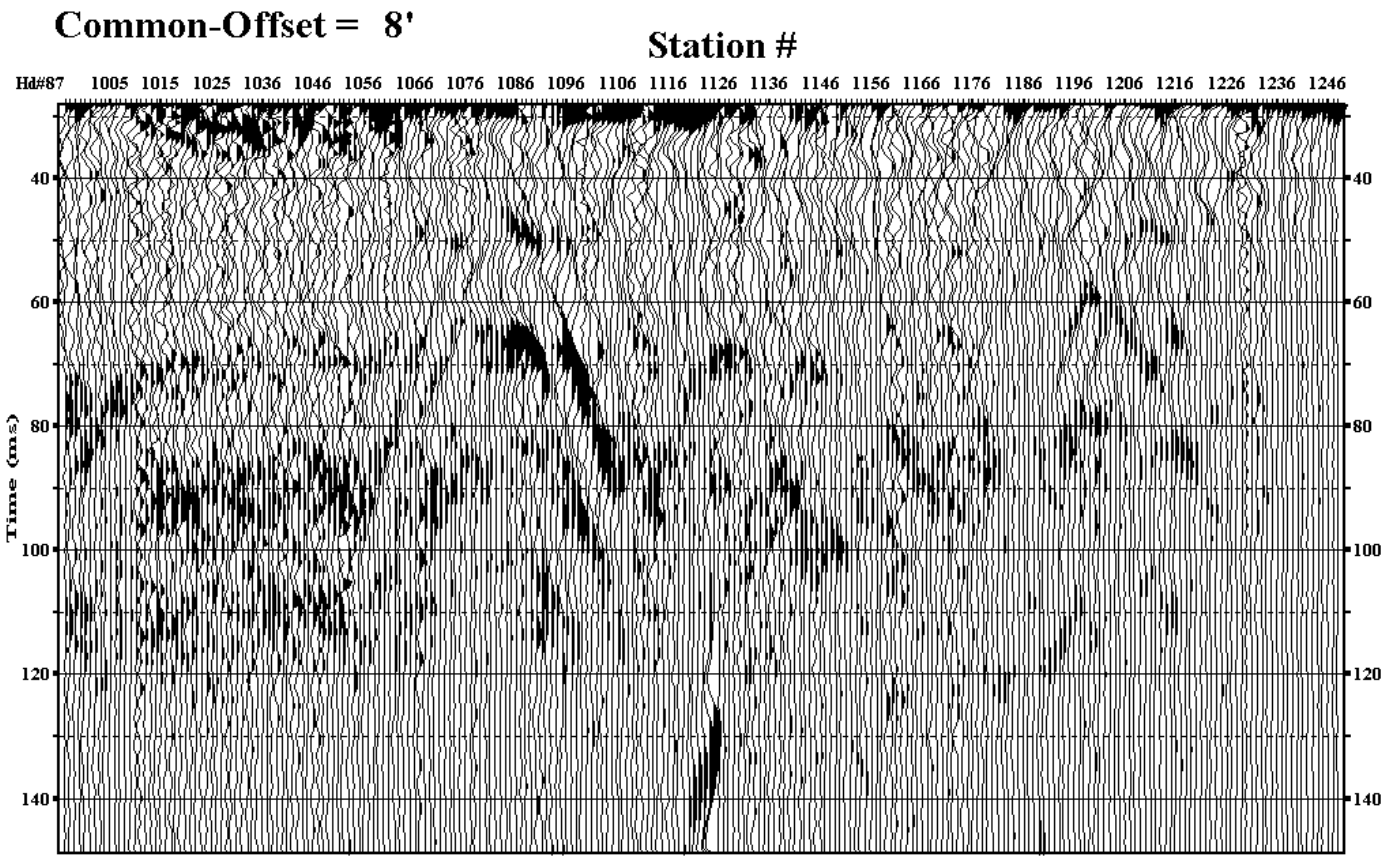

Figure 6. Common-offset (8 ft) section from line 1 of field records displaying enlarged portions of early arrivals of surface waves. Several "hyperbolic" moveouts are noticeable, indicating possible existence of voids or pipes. The strong hyperbolic moveout near station 1080 indicates the possible existence of a large-scale anomaly.

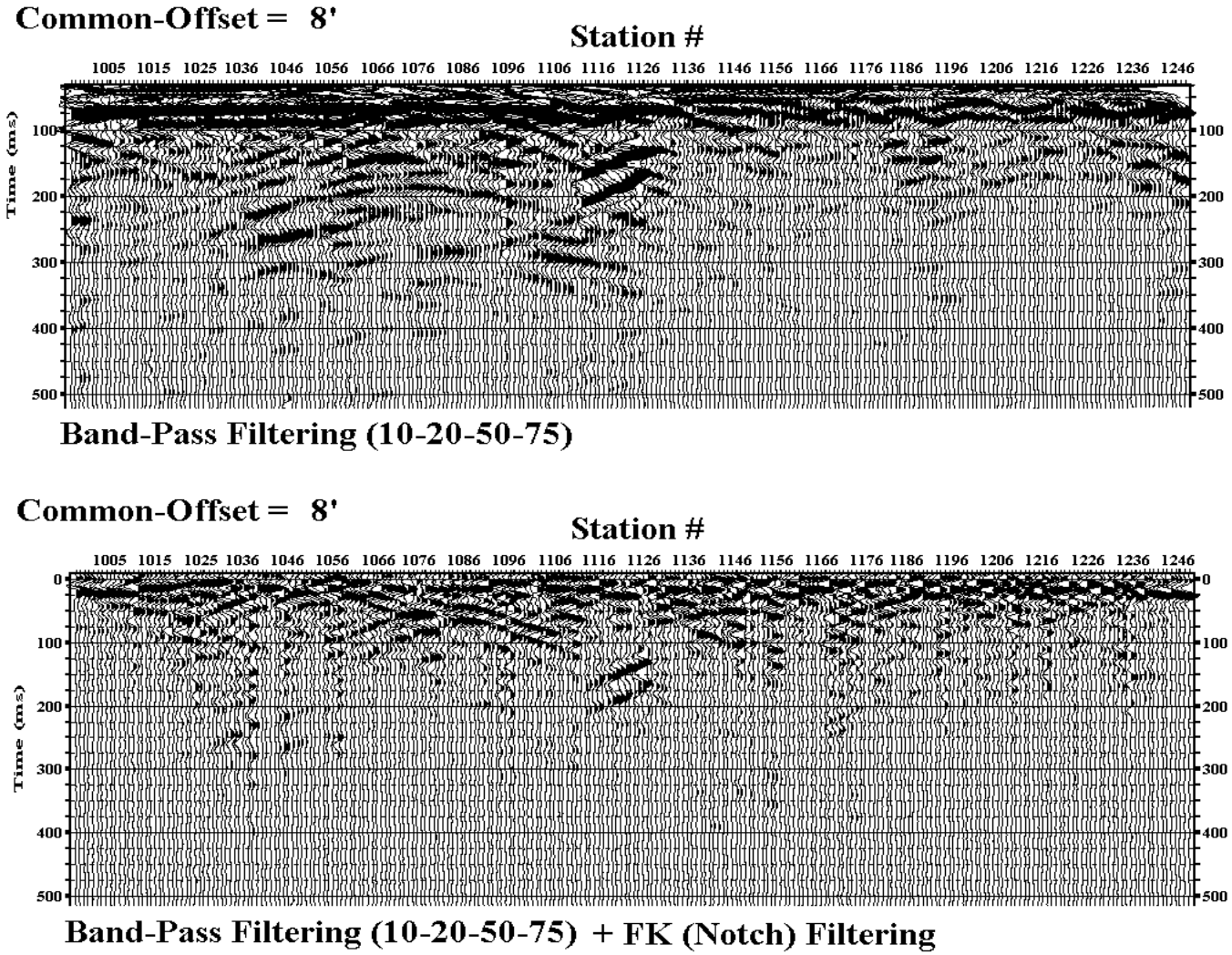

Figure 7. (a) Same common-offset section displayed in Figure 6 (after band-pass filtering has been applied) in decreased vertical scale. Many hyperbolic moveouts are noticeable. Calculation of the apparent velocity for all of the moveouts confirmed that all of them are surface-wave related events. The hyperbola near 200 ms indicates that it is the "off-line" scattering of surface waves. (b) F-K filtering of the section shown in (a) that filters out the horizontal coherent event and emphasizes the hyperbolic events.

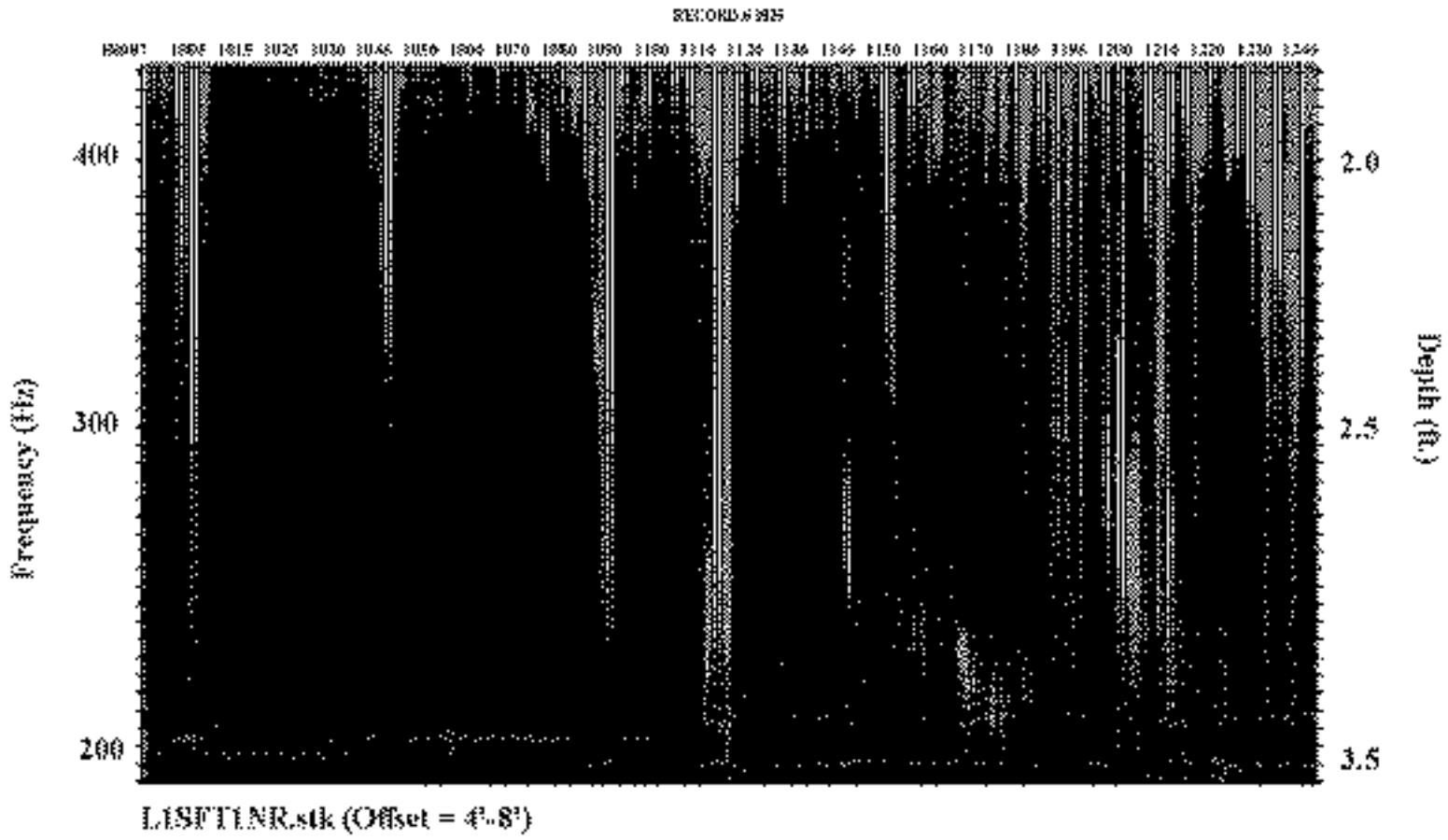

Figure 8. Wavefield transformation of shot gathers from line 1 similar to the section in Figure 6, but much higher frequencies (450-200 Hz) are used to focus in on the shallower (< 3.5 ft) part of the near surface.

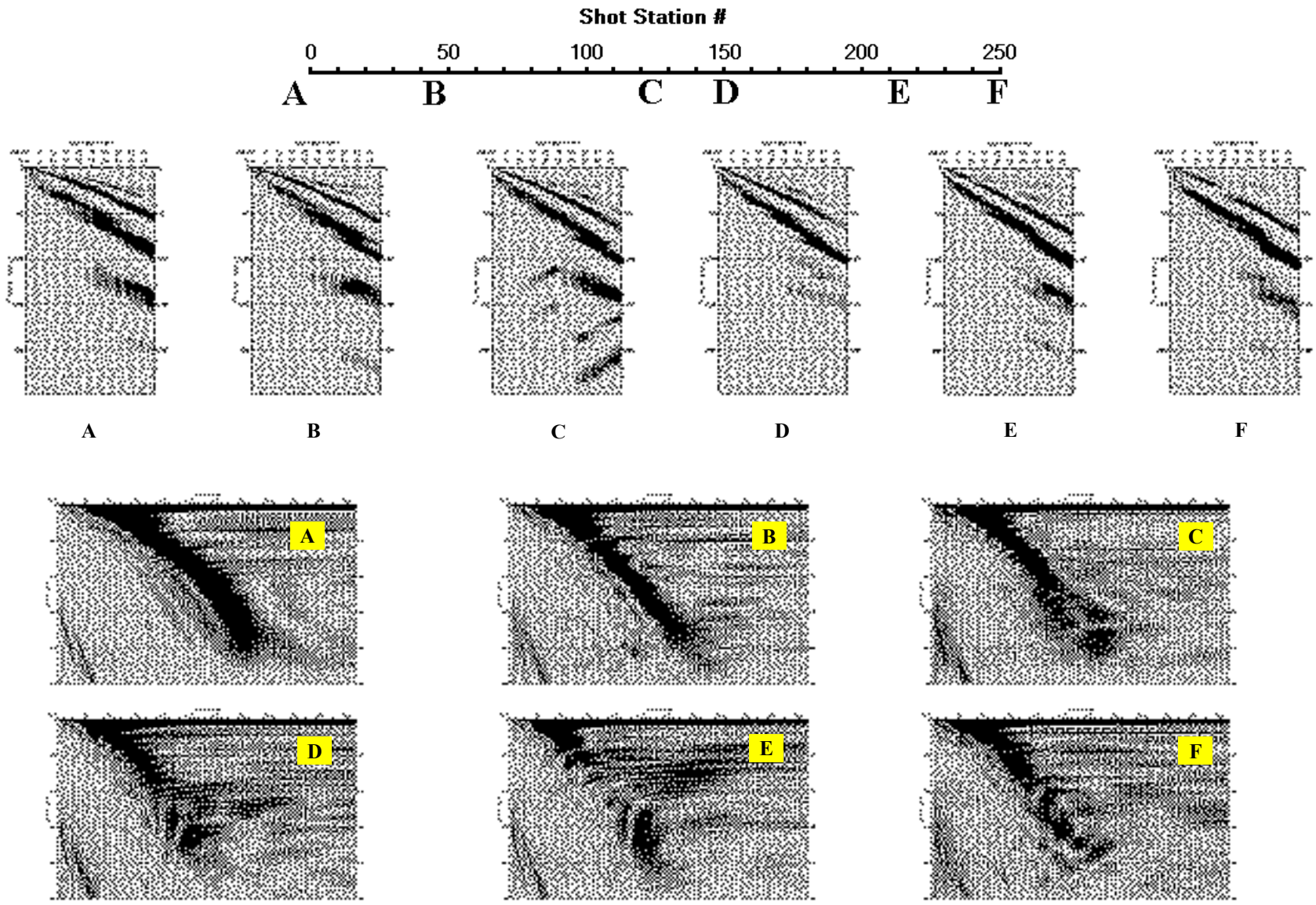

Figure 9. Shot gathers obtained at the marked shot stations (A-F) along the line and the corresponding dispersion curve images.

shear wave profiles. A single borehole exists near the eastern end of the profile. The profile was laid down in hopes of correlating the shear wave velocity field to data recorded from this borehole.

Data possessed a usable bandwidth of 5 Hz to 25 Hz, equating to a minimum and maximum depth of penetration around 9 ft to 100 ft, respectively. With a 15% accuracy of inverted S-wave velocities, 100 ft/sec or more changes are sufficiently above the average error to interpret as variability in geology. Since the contour interval was selected at 50 ft/sec, anomalies with closure on two or more contour lines are related to measurable changes in subsurface properties. Velocity trends along line 2 are laterally consistent, with no apparent change in depth to unique lithologic boundaries or notable changes in velocity that might be consistent with an anomalous subsurface (Figure 10). Line 2, at the resolution of these data, appears to have relatively uniform layering with several relatively small anomalous velocity zones within the upper 10 ft. When interpreting anomalies shallower than 10 ft it must be kept in mind that features less than 9 ft must be considered questionable when considering the sampling depth based on the half-wavelength axiom. It is interesting to note that at the very deepest part of the imaged section, especially on the smoothed versions of the section, a high velocity mound, possibly bedrock, is evident around station 1080 extending upward from below the imageable depth of this survey.

With little else in the way of anomalies on these data the high velocity mound beneath station 1080 represents the most interesting feature imaged (Figure 10). This “bedrock” high could easily act as a hydrologic barrier, inhibiting the east/west movement of fluids along the bedrock surface. The extremely localized nature of this high would have either not been sampled with grid drilling or it could have been extrapolated incorrectly in the surrounding area, making it out to be much larger than it really is. The zones of higher velocity materials in the very near-surface are quite small and must be evaluated with caution considering their depth. If they are real, based on their size and apparent contrast, they are likely related to differential compaction associated with the road, construction of the fence around the pits, or utilities that might have been buried along the road at one time.

Waveform transformations show little in the way of anomalous subsurface features with signatures that exceed background noise sufficiently to interpret on stacked shot gathers as related to geology and not noise (Figure 11). Several breaks in the otherwise laterally coherent frequency arrivals that penetrate to depths of around 15 ft can be observed beneath stations 1085

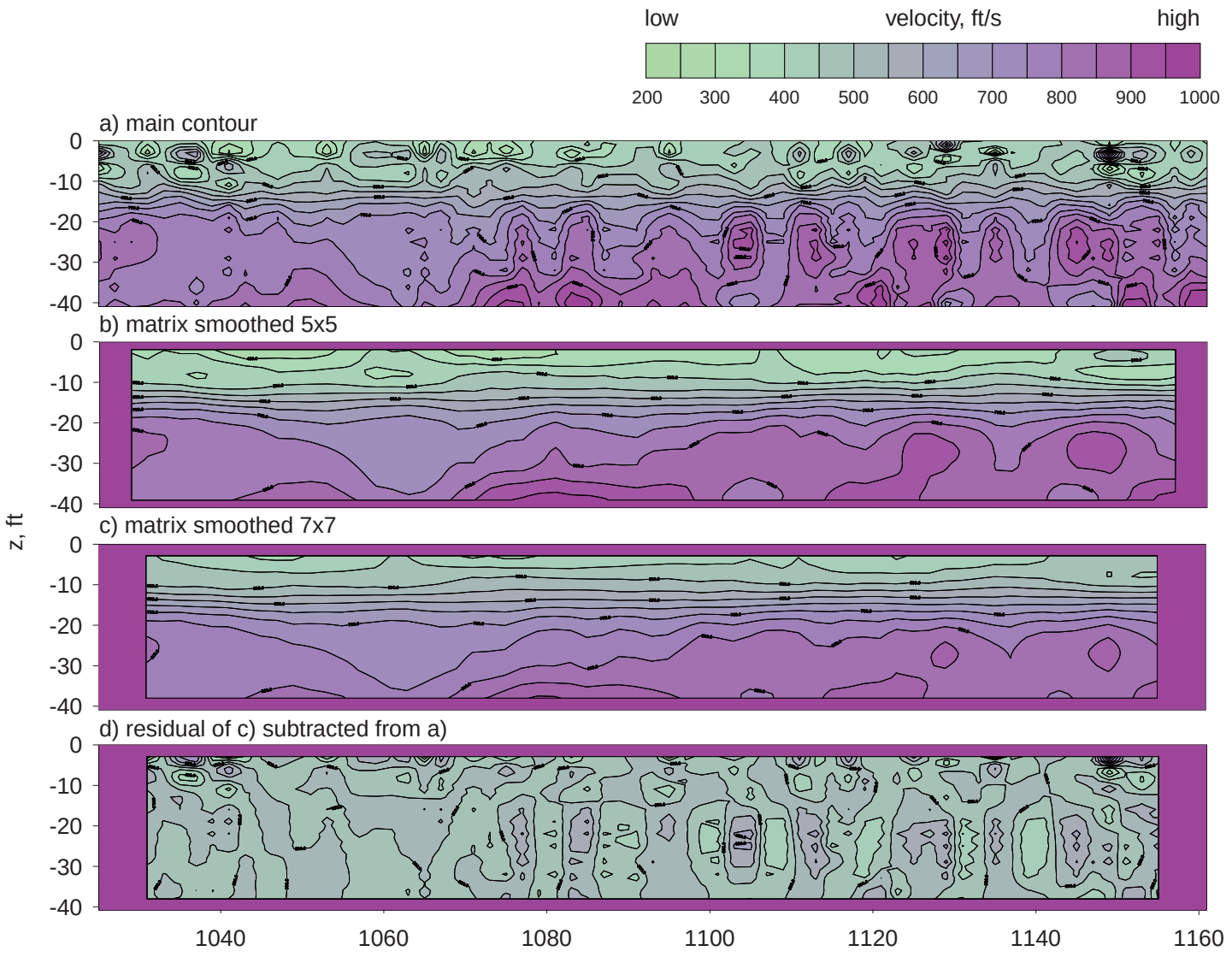

Figure 10A. (a) Shear wave velocity contour map of line 2 (b, c) with different degrees of smoothing applied and (d) residual.

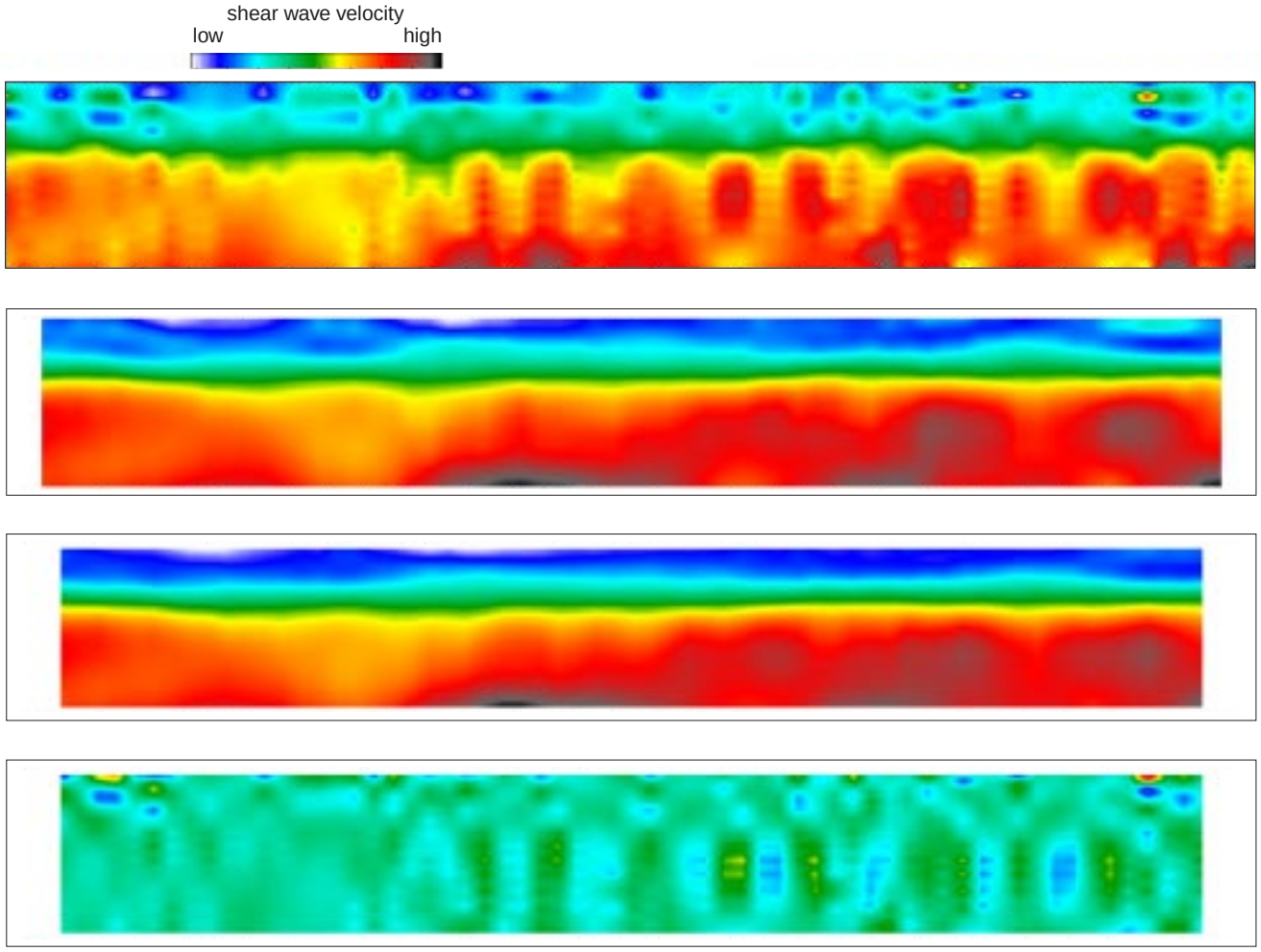

Figure 10B. Shear wave velocity contour color images of line 2 (data from Figure 10A).

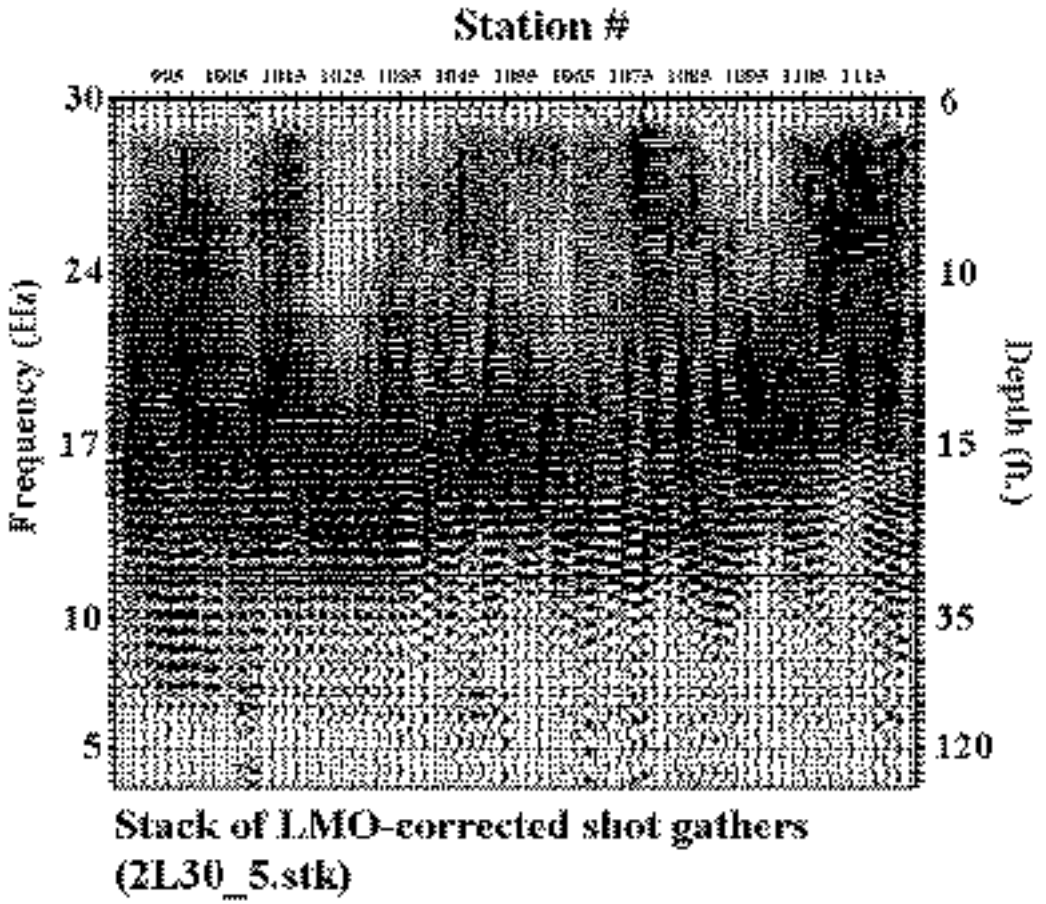

Figure 11. Wavefield transformation of shot gathers from line 2 similar to the section in Figure 4. The frequency range of the transformation was 30-5 Hz and the corresponding depth range is approximately 5 ft to 120 ft.

and 1120 on CMP gathers (Figure 12). Without drill investigations neither of these would justify a definitive interpretation. With the uniformity of the frequency signatures of energy on either side of the anomaly at station 1085 within the frequency range of 15 to 20 Hz, it is more reasonable to suggest this wavefield disturbance is related to real geology. The feature beneath station 1120 seems to mark the beginning of a transition into an area with a different apparent linear surface wave moveout and little or no frequency content below 15 Hz and is, therefore, most likely an edge effect resulting from our acquisition geometry. It is very evident on common offset sections that the wavefield in this area is relatively undisturbed, indicative of a laterally continuous subsurface (Figure 13).

SITE 3—South to North line on dike, through tar pits

Seismic data for site 3 were collected starting near the railroad tracks immediately south of the tar pits, extended north along the dike separating the two pits, and ended near the northern end of the westernmost pit (Figure 1). The line was acquired completely on grass, dirt, or gravel road, permitting use of traditional spikes along the entire line. The source was an accelerated weight drop mounted on a four-wheel drive tracked vehicle. Geophones were spaced at 2 ft with a source-to-nearest-receiver offset of 24 ft. The objective of this profile was to evaluate the effectiveness of the method to distinguish the base of the man-made dike built to separate the two pits. Maximum depth of penetration based on the half wavelength axiom within the highly reliable portion of the spectrum was around 35 ft along this profile. A secondary objective of this profile was to examine any bedding geometry beneath the base of the dike. Line 3 intersected line 2 at around station 1030; however, due to the acquisition geometry and presence of the railroad embankment, the tie point was at the extreme end of the profile and cannot be correlated to line 2 at that intersection with much confidence.

Data possessed a usable bandwidth from 5 Hz to 50 Hz, which equates to a minimum and maximum depth of penetration of around 4 ft to 120 ft, respectively. As with previous lines, due to the accuracy of inverted S-wave velocities, closures defined by a single contour are not sufficient to interpret with the confidence required for this survey and are considered background and used only to establish velocity trends. Velocity trends along line 3 are laterally consistent, with only uniform variations across the profile. Of particular interest on line 3 is the presence of a shallow low velocity zone on the southern end of the line that is particularly evident on the

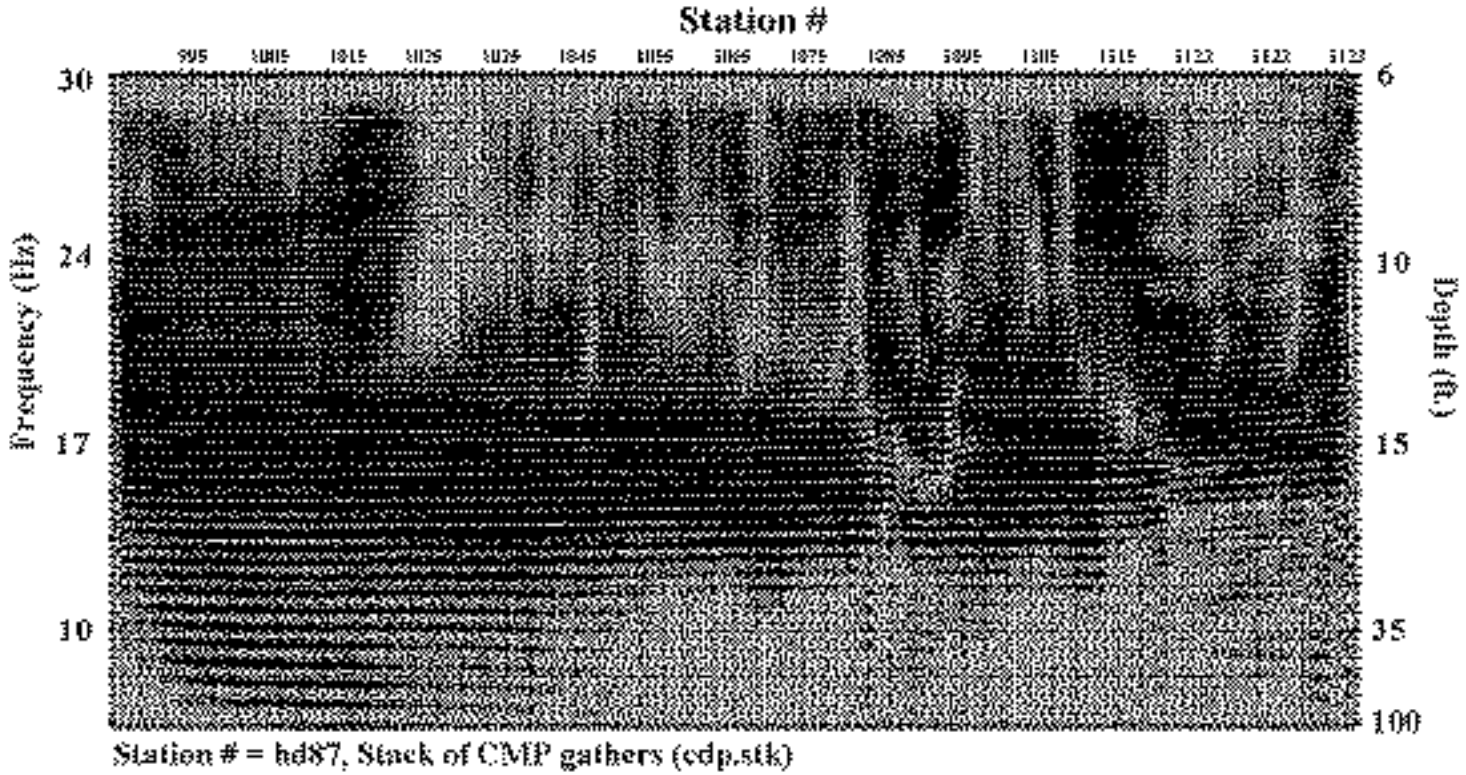

Figure 12. Wavefield transformation of CMP gathers from line 2. This section, in theory, has higher horizontal resolution than the wavefield transformation of the shot gathers shown in Figure 11.

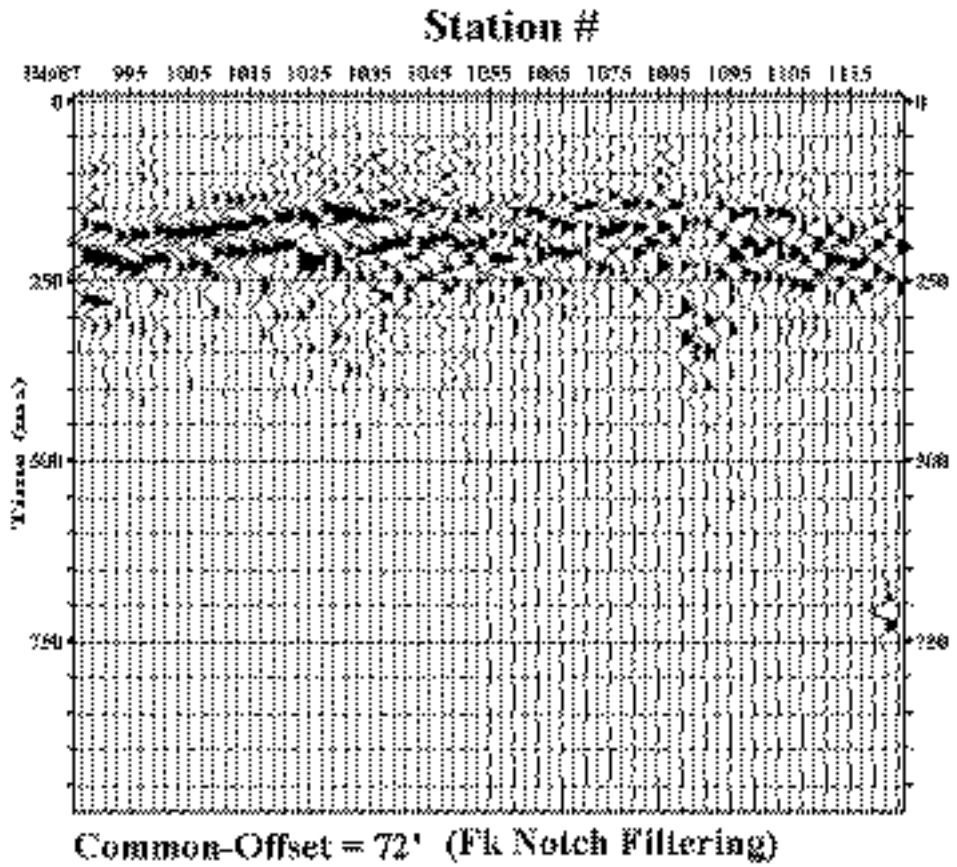

Figure 13. Common-offset (72 ft) section of field records from line 2 after F-K filter has been applied to filter out the horizontal event in order to emphasize any hyperbolic events.

smoothed section (Figure 14). This low velocity zone extends to a depth of around 8 to 10 ft near the south end of the profile, tapering to depths of less than 4 ft near station 1120. This wedge-shaped layer is likely consistent with the dike. Data north of about station 1130 is probably sampling the portion of the dike less than 2 ft thick and thinning to be consistent with the original ground surface near the northern end of the profile.

Of secondary interest is the channel or basin-like bedding geometry coincident with the thicker portion of the dike that appears to be present on the south end of the line. This channel feature is enhanced on the smoothed versions of the data. The channel feature appears to extend to depths of about 25 ft beneath station 1120 and 20 ft beneath stations 1035 and 1135. The northern end of the channel or bowl feature has the steepest dip, indicating a channel feature that is elongated to the south (at least in the two dimensions imaged by this survey). Also of interest beneath line 3 is an apparent rise in bedrock near the northern end of the profile. With the apparent bedrock mound interpreted on line 2 and now a similar velocity feature on line 3, it is possible to begin speculating about the general configuration of the bedrock surface. As on line 2, depending on the near-surface geology, the bedrock high on line 3 could impact the dynamics of the hydrology in this area.

Consistent with line 2, waveform transformations of line 3 show very little in the way of anomalous subsurface features with signatures that could be interpreted as related to geology and not background noise on stacked shot gathers (Figure 15). Linearly moved-out shot gathers from this line possess no significant breaks in the waveform at any frequency component across this profile when stacked and displayed in a cross-sectional format. Data processed and displayed in this format will be sensitive to very localized anomalous zones. There were no expectations that such zones existed beneath this line, but this would provide some insight into the issue of compaction within the basin. It is very evident on both the CMP stacked section (Figure 16) and common offset section (Figure 17) that the wavefield in this area is relatively undisturbed, indicative of a laterally continuous subsurface. Of minor interest yet noteworthy is the very subtle decrease in amplitude of high-frequency arrivals beneath station 1020 and again between stations 1047 to 1057 (Figure 16). These features are evident on common offset sections as velocity decreases (Figure 17) and likely indicative of an anomalous zone (possibly undercompacted) within the fill composing the dike. From previous experience it is most likely

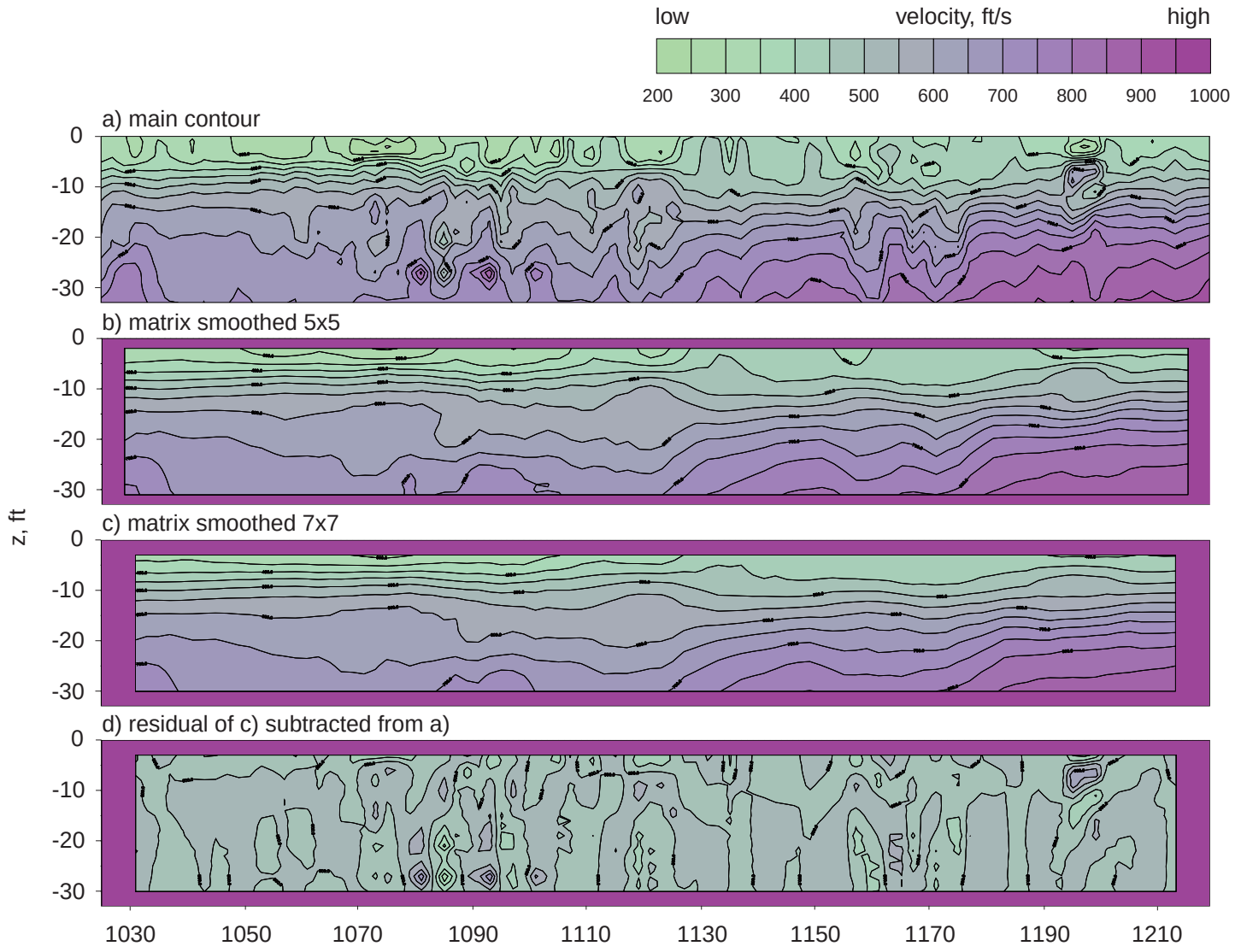

Figure 14A. (a) Shear wave velocity contour map of line 3 (b, c) with different degrees of smoothing applied and (d) residual.

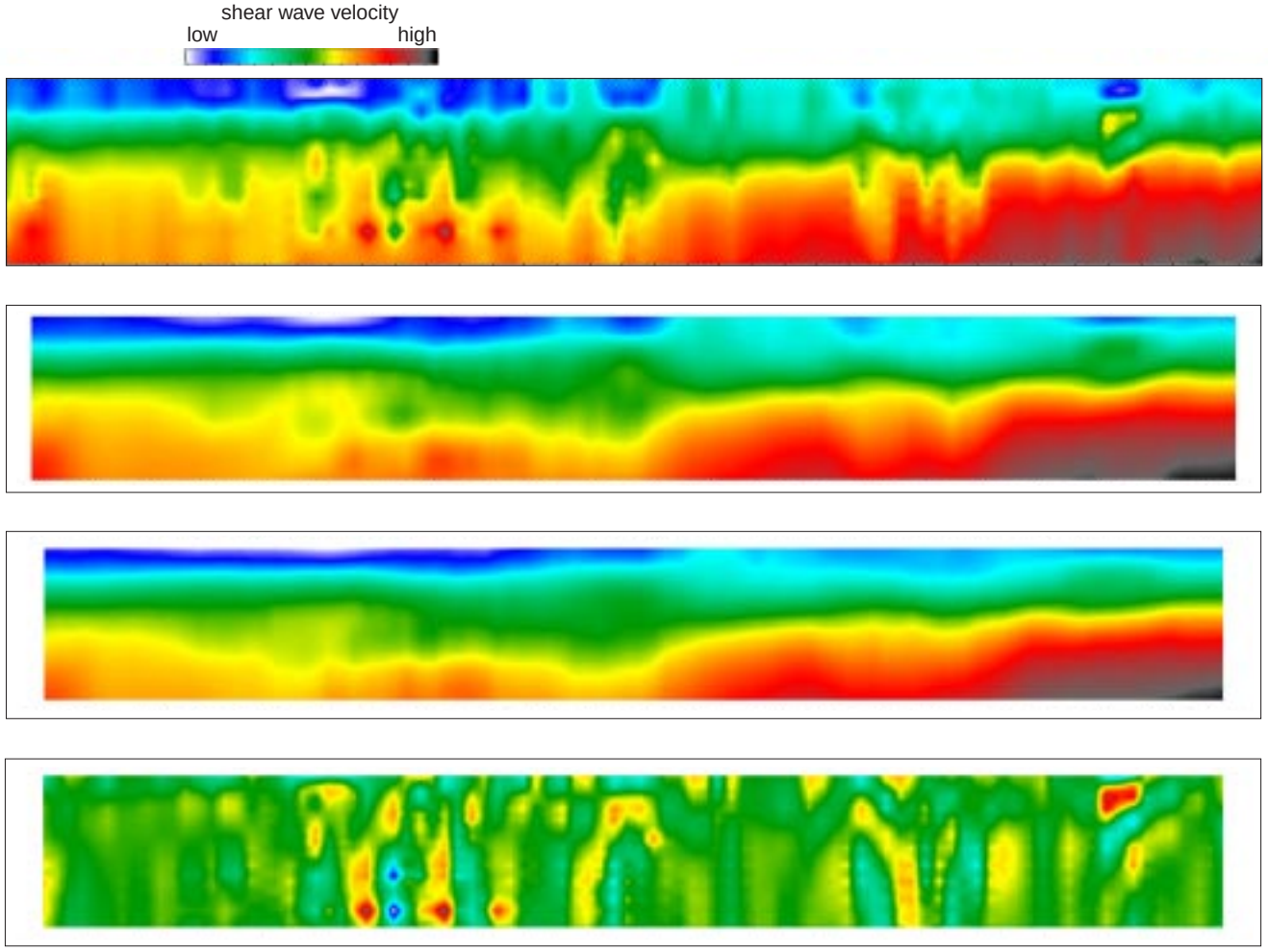

Figure 14B. Shear wave velocity contour color images of line 3 (data from Figure 14A).

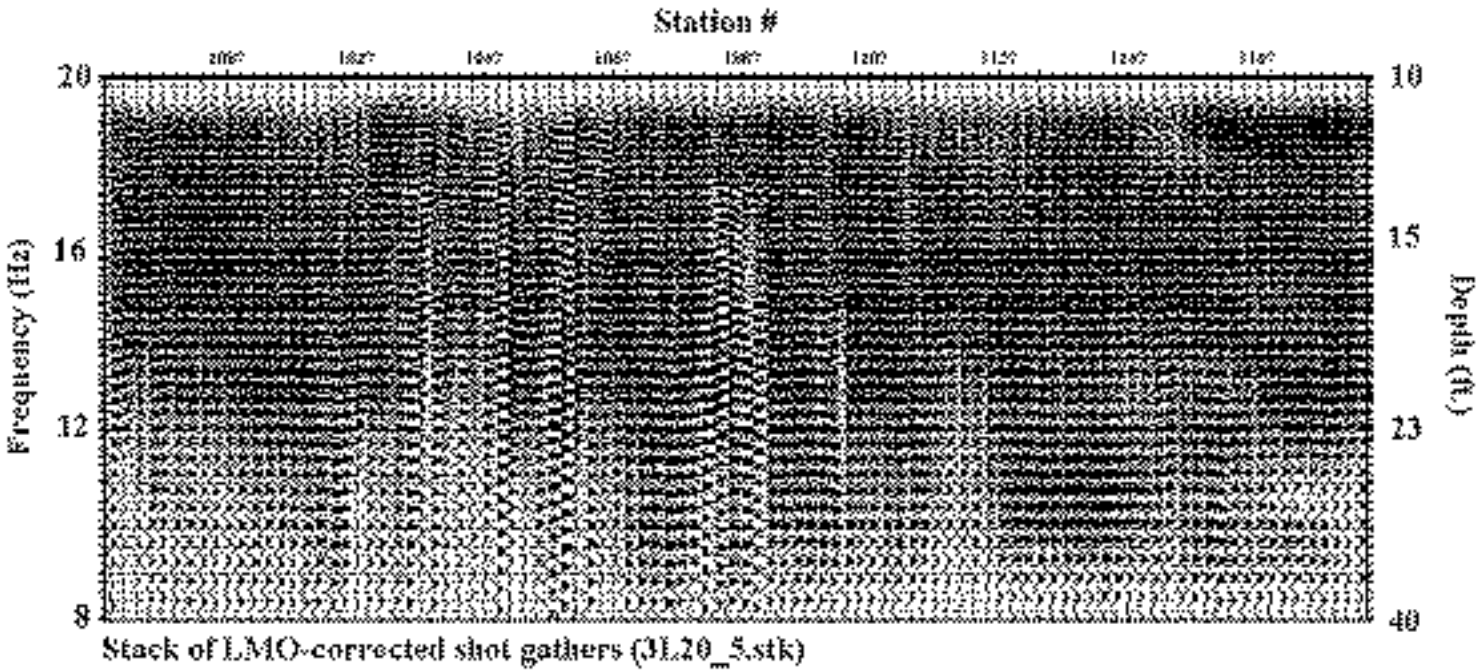

Figure 15. Wavefield transformation of shot gathers from line 3 similar to the section in Figure 4.

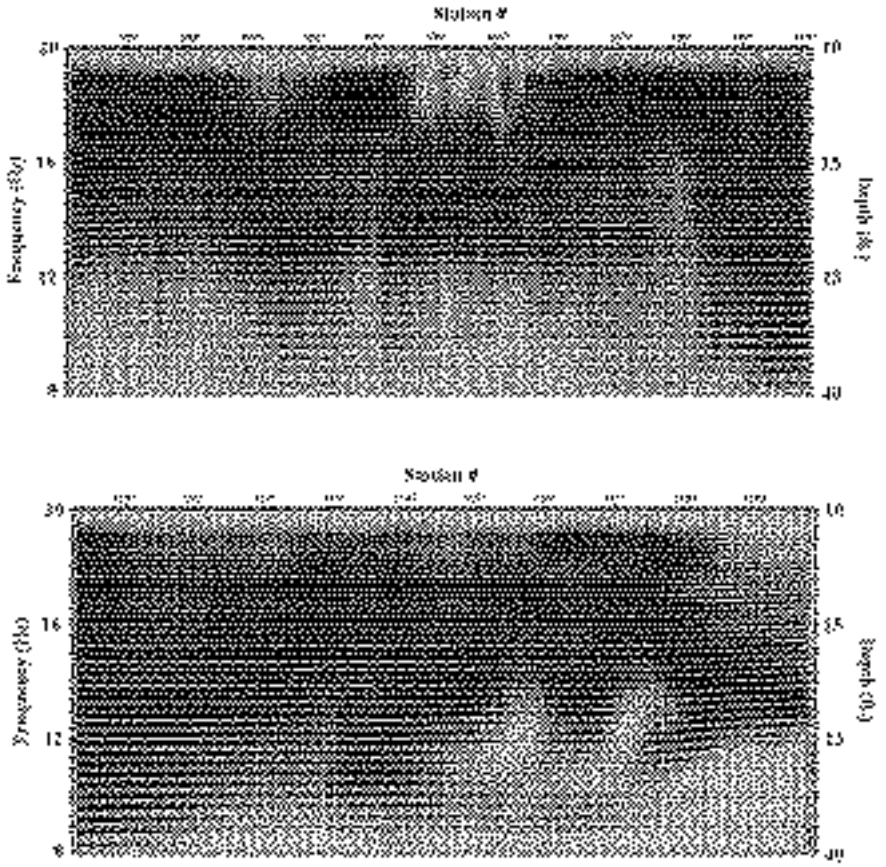

Figure 16. Wavefield transformation of CMP gathers from line 3. One section was segmented into two pieces for display purposes.

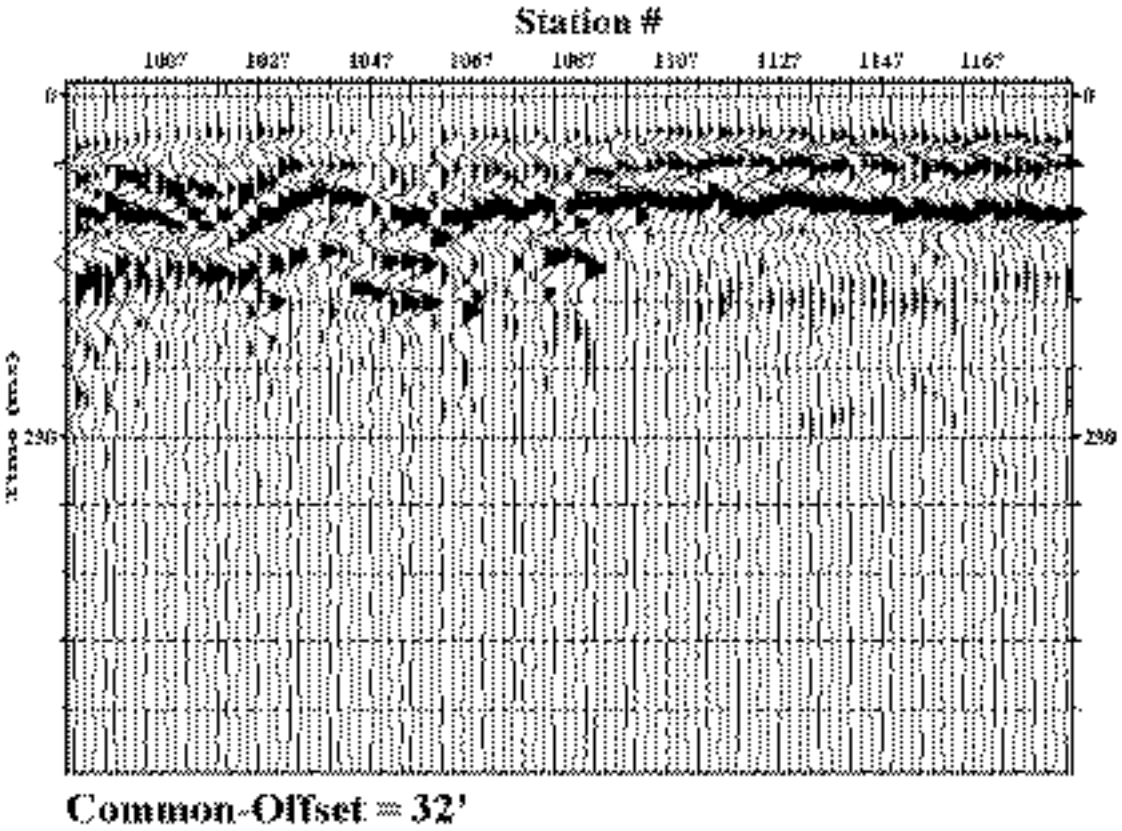

Figure 17. Common-offset (32 ft) section of field records from line 3.

these amplitude dropouts are the result of a decrease in shear wave velocity or density, likely representative of either dissolution, undercompaction, or non-native earth fill (rubble or refuse).

SITE 4—West of river and immediately east of refinery structures

Seismic data for site 4 were collected starting very near a well located immediately west of the river in an area on the eastern edge of the refinery previously used as a landfill (Figure 1). The line was acquired completely on grass and dirt, permitting use of traditional geophone spikes across the entire line. This line was positioned to cross directly over areas where pits were known to have existed at one time. Placement was guided by large patches of bare ground where no vegetation would grow. The source was a 20 lb sledgehammer impacting a 1 sq ft aluminum plate on 4 ft intervals along the profile. The geophone spacing was 2 ft with a 24 ft source-to-nearest-receiver offset. The objective of this survey was to evaluate the utility of this method to delineate buried pits and capped landfills which had been abandoned and covered with native materials for several years. Maximum depth of penetration based on the half-wavelength axiom was around 30 ft along this profile. However, from empirical observations it is unlikely anything meaningful can be interpreted from depths exceeding 20 ft BGS. A secondary objective of this profile was to evaluate the potential of mapping the geometry of unconsolidated material bedding beneath the pits. A boring located at the extreme east end of the profile does not tie directly to the processed line as a result of the acquisition geometry and the river bank, which limited the distance the line could extend to the east.

Data possessed a usable bandwidth of 10 Hz to 70 Hz, equating to a maximum and minimum depth of penetration around 25 ft to 2 ft, respectively. As on previous data, anomalies with closure on two or more contour lines are related to measurable changes in subsurface properties, while localized closures defined by a single contour may be related to geology, but are below the required level of certainty on this study. Velocity trends along line 4 are laterally uniform, and in general, consistent with a very homogeneous subsurface across the profile. Of particular interest on line 4 is the presence of localized high and low velocity closures near the eastern end of the profile (Figure 18).

The anomalous zones, such as those observed on the velocity contoured section, are conceptually consistent with a variety of materials placed in a surface-compacted (capped) landfill or an infilled burial pit (Figure 18). Based on the gradient and absolute value of the

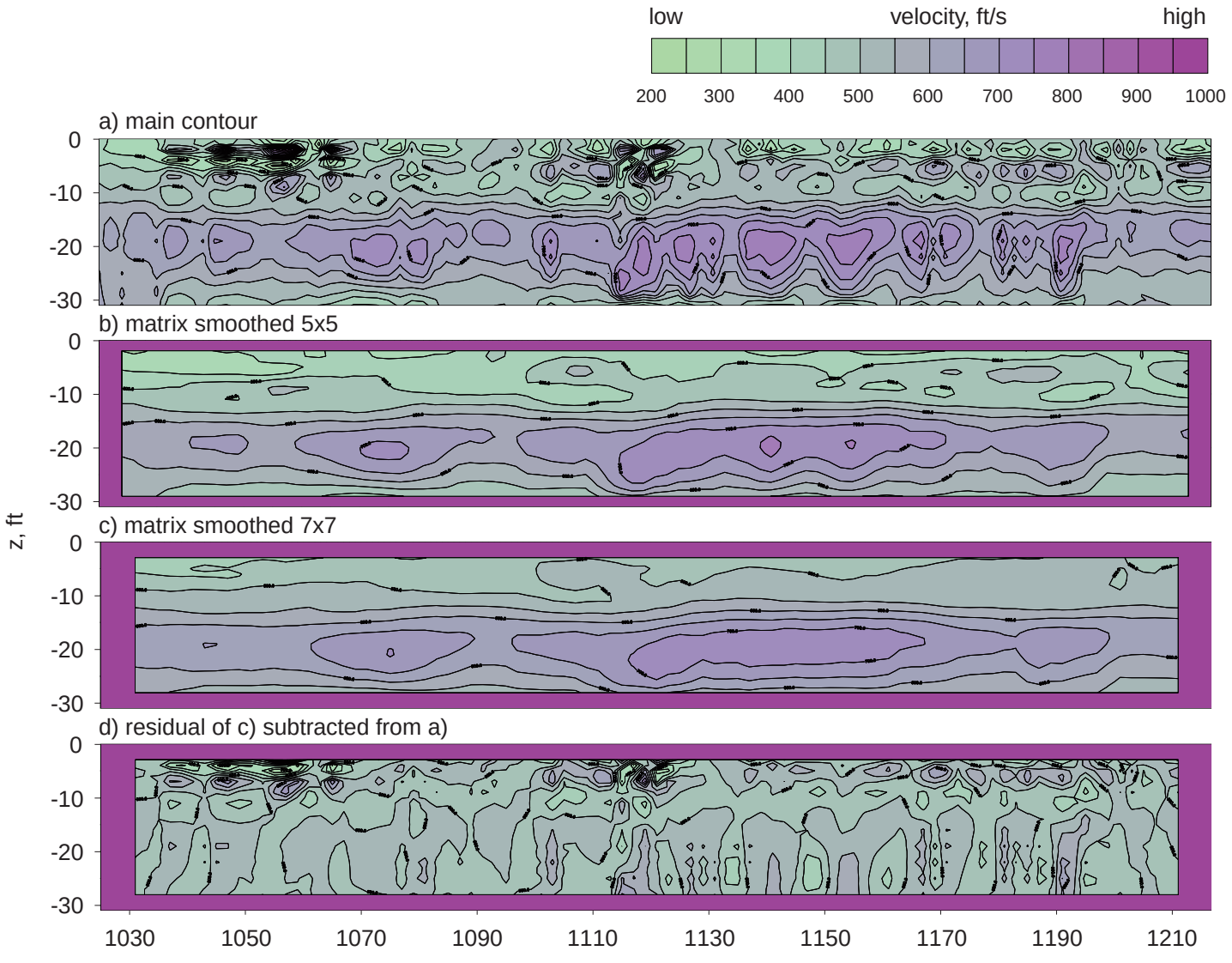

Figure 18A. (a) Shear wave velocity contour map of line 4 (b, c) with different degrees of smoothing applied and (d) residual.

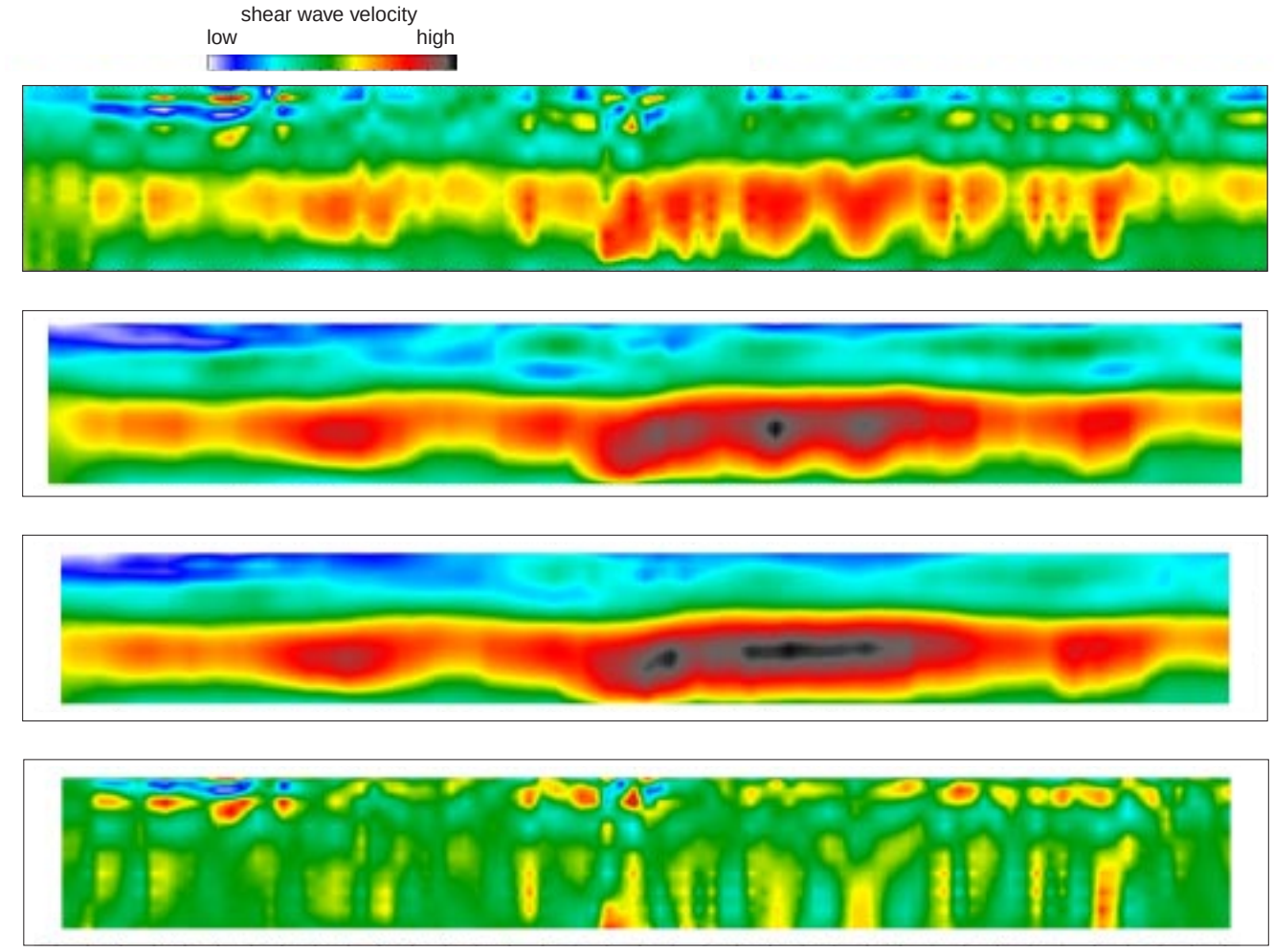

Figure 18B. Shear wave velocity contour color images of line 4 (data from Figure 18A).

anomalies on the east end of the profile, it is reasonable to suggest that natural sediments present at depths from 2 to 8 ft prior to refinery activities beginning at this site have been altered or replaced beneath stations 1035 to 1060. It is not possible to speculate on how this area might be disturbed, or even if it is natural (river channel) or manmade (landfill), however it is quite likely considering the character, gradient, and location of this feature, it is an acoustic expression of an old trench. Looking deeper into the section, a high velocity zone can be interpreted beginning at a depth of around 15 ft and extending below the imageable depth of this survey. As stated previously, the maximum depth interpretations can be made with any confidence is around 20 ft. The apparent velocity inversion below about 25 ft results from insufficient low frequency energy penetration to that depth. The high velocity layer is likely a relatively tight clay or silty-clay, or possibly the boundary between alluvial sediments and glacial materials.

Waveform transformations of line 4 possess a unique character that is clearly diagnostic of either two large areas with disturbed subsurface as evidenced by the dramatic drop in the amplitude of surface wave energy, or one large disturbed subsurface area as evidenced by the dramatic increase in the amplitude of surface wave energy (Figure 19). It would be quite speculative to suggest the apparent anomalies on the linear moveout sections (Figures 19 and 20) are real considering the signal-to-noise ratio of the upper 4 ft at this site (Figure 19a). Clearly from 50 Hz and higher, 50% or more of the recorded energy is noise (or in this case, body or air waves). Since that is the case, it is only reasonable to attempt interpreting anomalies deeper than 4 ft BGS. This being said, the trench feature at the eastern end of line 4 on the velocity contour data is at the limits of what should be interpreted with any degree of confidence using these data. An interesting phenomenon on the common offset gathers of these data is the appearance of diffraction-looking arrivals beneath stations 1047 and 1087 (Figure 21). These features are most likely reflected groundroll and could be indicative of an abrupt change in the velocity of near-surface materials perpendicular to the plane of the surface wave, such as a pit wall.

SITE 5—North to South line along east berm of land farm

Seismic data for site 5 were collected from the gate at the northeastern entrance to the land farm to the northeastern edge of the tank farm (Figure 1). The entire line was collected on top of the berm marking the eastern boundary of the land farm. Shot and receiver stations were on top of the berm and therefore elevated approximately 5 ft above the native ground surface,

(a) (b)

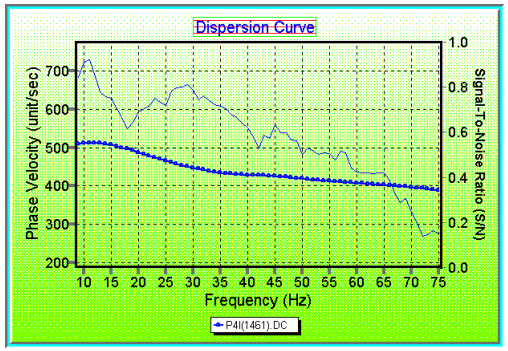

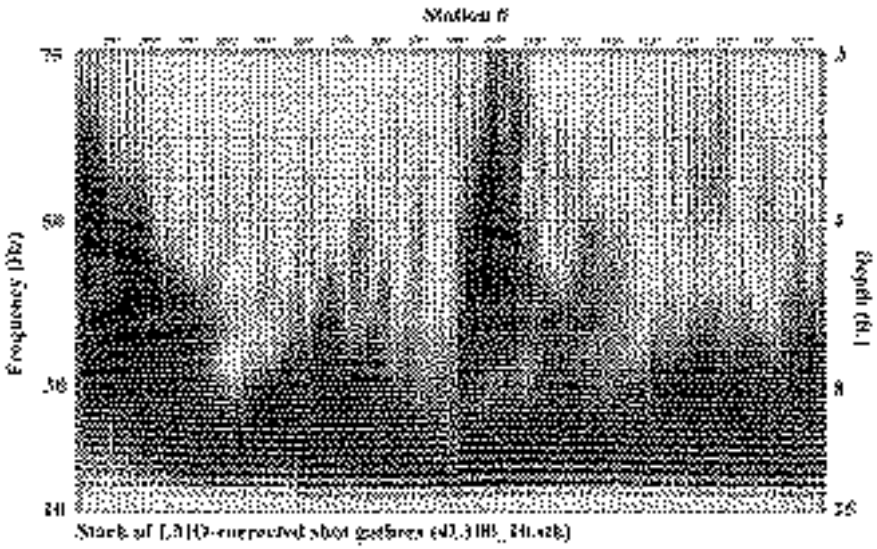

Figure 19. (a) A typical display of dispersion and S/N curves for line 4. (b) Wavefield transformation of shot gathers from line 4 similar to the section in Figure 4.

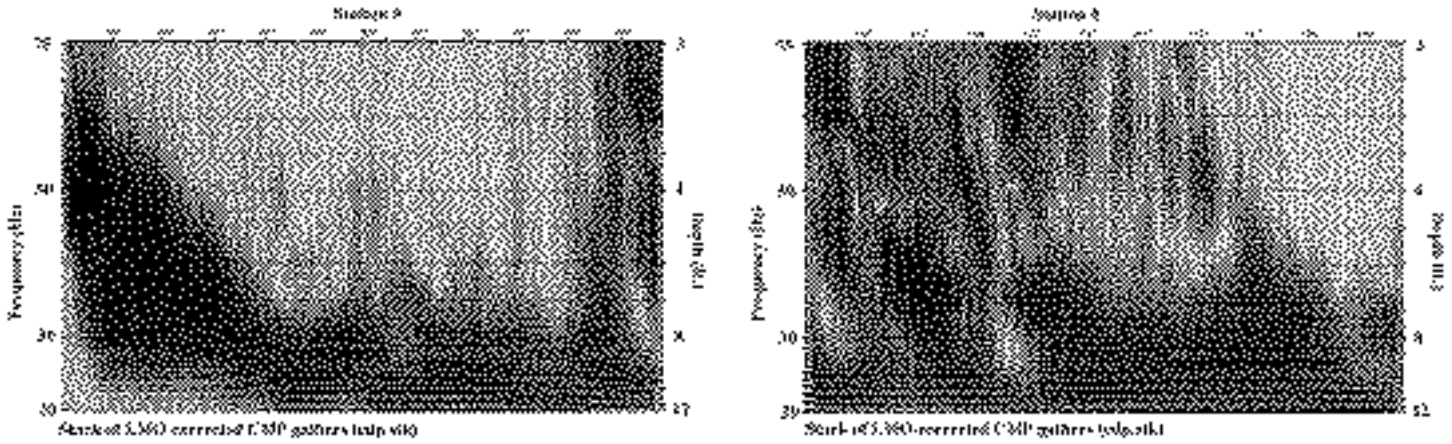

Figure 20. Wavefield transformation of CMP gathers from line 4. One section was segmented into two pieces for display purposes.

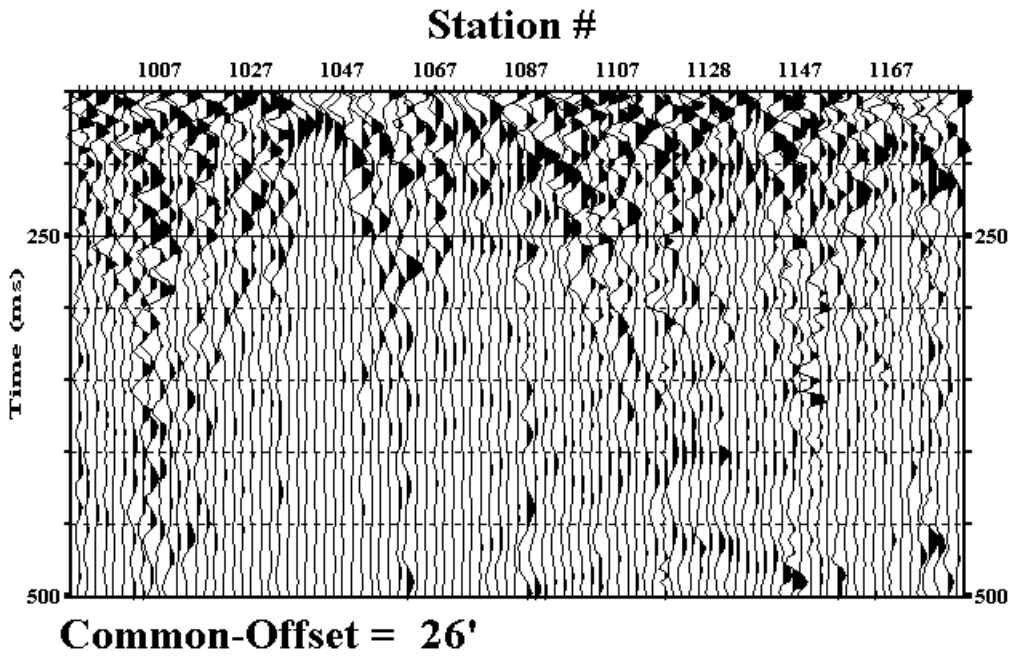

Figure 21. Common-offset (26 ft) section of field records from line 4.

coincident with the western edge of the berm. The line was acquired completely on grass, permitting use of traditional geophone spikes along the entire line. The source was an accelerated weight drop mounted on a four-wheel drive tracked vehicle, vertically stacking 3 impacts every 8 ft. Geophone spacing was 4 ft with a 56 ft source-to-nearest-receiver offset. The goal of this survey was to evaluate the effectiveness of this method in delineating as many distinct layers of alluvial or glacial material as possible, and as deep as possible, above a bedrock surface proposed to be over 100 ft BGS.

Maximum depth of penetration based on the half wavelength axiom was around 100 ft along this profile. Subsurface layers, down to 100 ft BGS are relatively flat lying with only minor topographic variations (Figure 22). Three distinct layers appear interpretable along the profile. The shallowest one extends to a depth of 15 to 20 ft. This layer seems to possess more lateral variability in material properties than deeper units. This observation is not at all unexpected, and quite reasonable, considering the relative difference in age and compaction of the shallower sediments in comparison to those at 20+ ft burial. The second packet of layers extends from about 20 to depths of 80 to 90 ft. This unit is characterized by extremely gradual and uniform increases in shear velocity, a likely indicator of grading sequences of gravels, sands, and silts. The deepest layer could be bedrock or at least a significantly higher shear wave velocity material such as glacial tills with alluvial sequences above. It appears to have a local high (topographic) beneath station 1130. The surface has the appearance of being erosional in nature with several marked irregularities. All things considered, data obtained along this line results in a processed section that is well within expectation.

Data possessed a usable bandwidth of 5 Hz to 25 Hz, equating to a minimum and maximum depth of penetration around 10 ft to 100 ft, respectively. Velocity trends along line 5 are laterally consistent, with very uniform and grading variations across the profile. Of particular interest on line 5 is the presence of the higher velocity, structural high beneath station 1130 (Figure 22). A complex series of velocity gradients are evident within the upper 10 to 20 ft along portions of this profile (Figure 22). These features are quite consistent with an active alluvial plain. Sufficient high frequencies and close offsets were not available to allow the confident imaging of the base of the berm.

Waveform transformations of line 5, as with lines 2 and 3, show very little in the way of anomalous subsurface features (velocity closures) with signatures that could be interpreted as

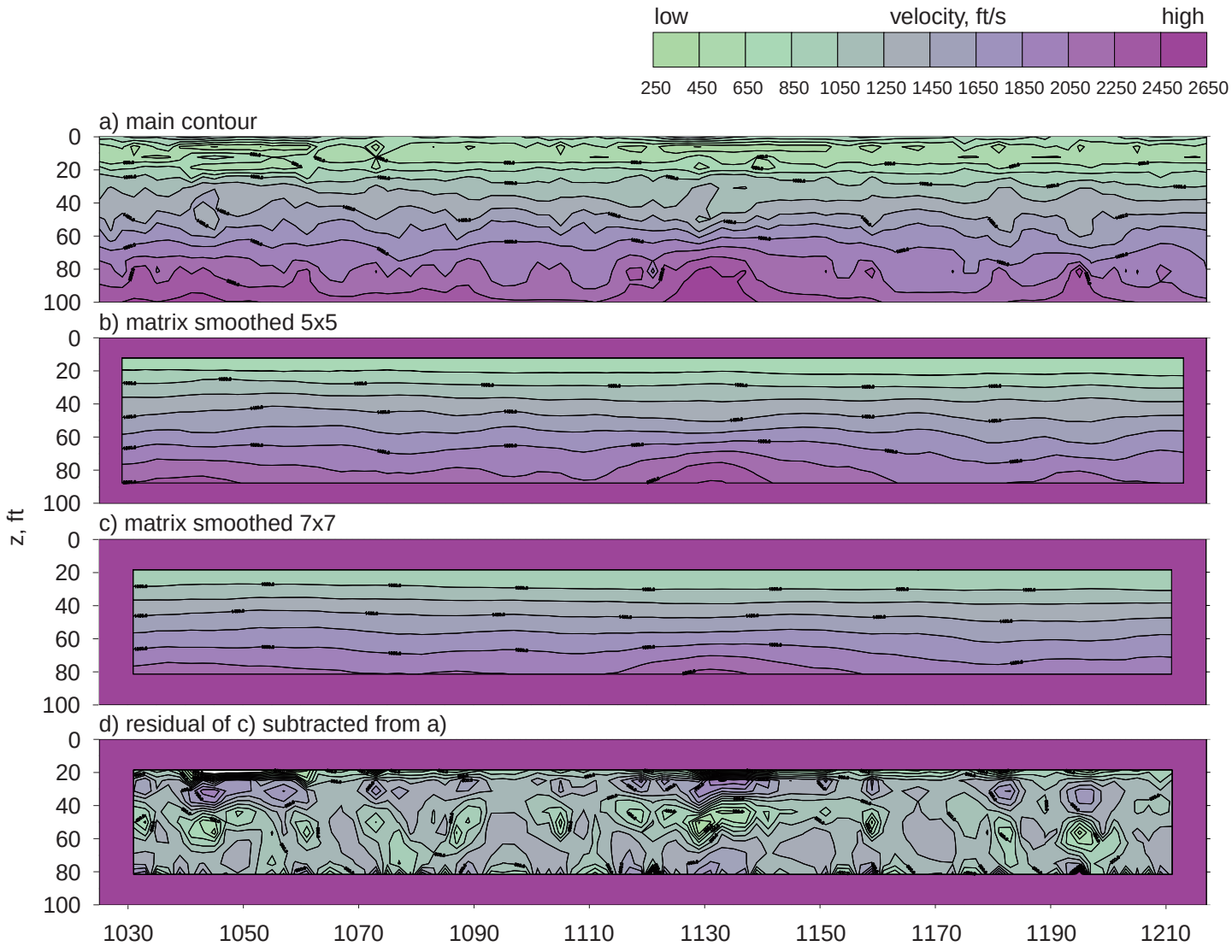

Figure 22A. (a) Shear wave velocity contour map of line 5 (b, c) with different degrees of smoothing applied and (d) residual.

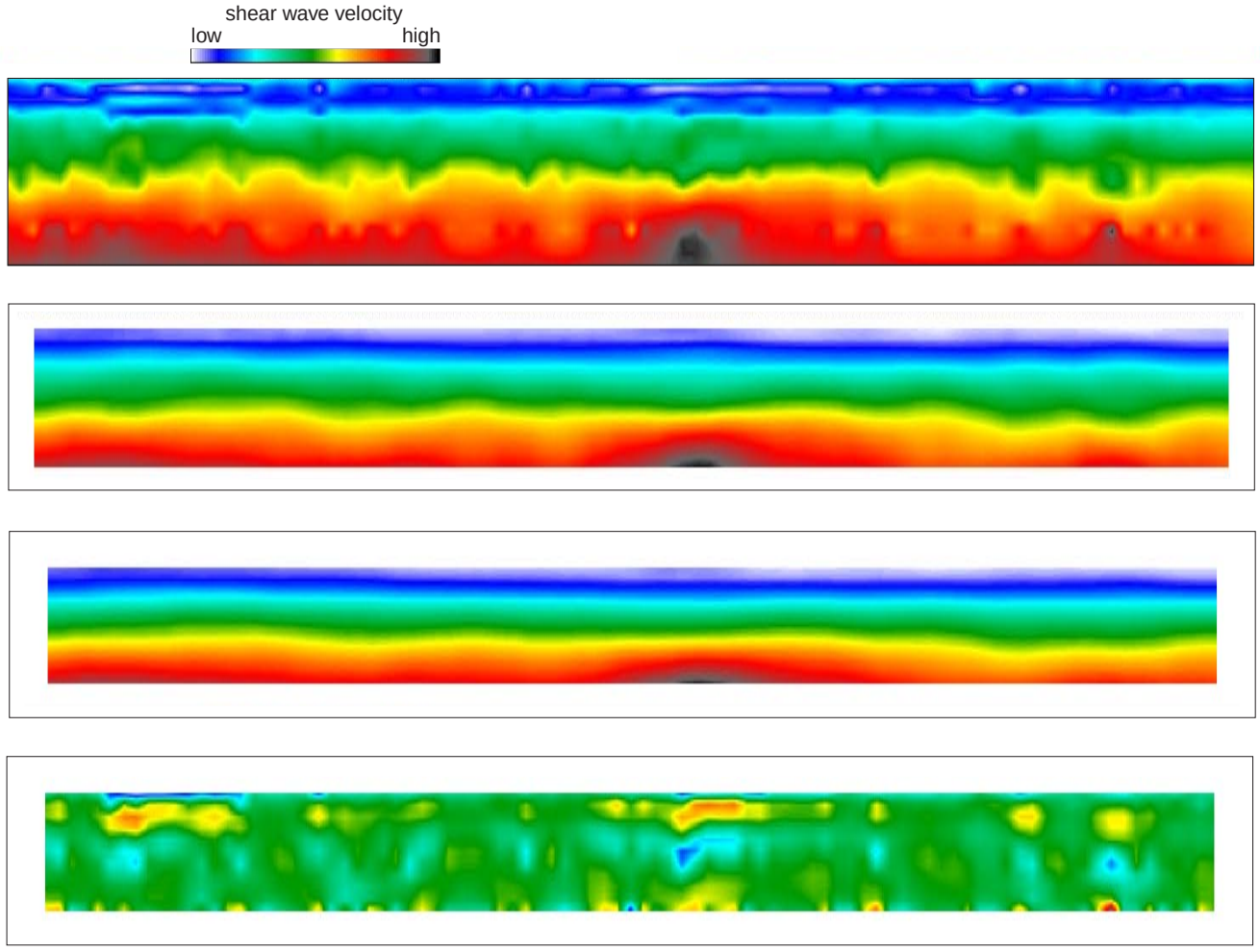

Figure 22B. Shear wave velocity contour color images of line 5 (data from Figure 22A).

related to geology and not background noise on stacked shot gathers (Figure 23). Linearly moved-out shot gathers, when stacked and displayed in a cross-sectional format, possess no significant breaks in the waveform at any frequency component. However, the shot gather stacks do suggest that a 2 to 3 ft thick layer distinctly different from those above and below is present at around 15 ft BGS. This depth is consistent with the boundary between the first and second layer as interpreted on the velocity contour data. It is possible to speculate that the minimal amplitude returns from depths between 7 and 10 ft could be the base of the berm. Caution must be exercised when interpreting layers above 10 ft, considering the frequency content of the data. It is likely the berm was built after the removal of the upper 3 ft of soil. In that case, the base of the berm would be at a depth of around 7 to 10 ft. Of course, data displayed using amplitude and phase variations will be most sensitive to very localized changes in material, especially where velocities changes are relatively rapid. It is obvious on both the CMP stacked section and common offset section that the wavefield in this area is undisturbed, indicative of laterally continuous subsurface layers changing very gradationally with depth (Figures 24 and 25).

Conclusions

Shear wave velocity field data provides insight into changes in subsurface materials at all five of the sites studied. The shear wave velocity was relatively consistent as a function of depth at all sites. Depths of energy penetration were dependent on the acquisition geometry and frequency band of the surface wave energy. In general, it was possible to resolve three distinctly different velocity groups across the entire refinery site: a relatively variable sequence of sediments with evidence of anomalous materials or significant lateral changes in material properties generally extended from the surface to 10 to 15 ft BGS, a second zone of material seemed to be locally present from around 10 to 15 ft deep to in some cases depths of 80 to 90 ft BGS, and finally higher velocity materials were present on data penetrating depths over 30 ft BGS. It is very likely that these three distinct packets of velocities (materials) could be correlated around the entire refinery.

Based on the tests undertaken at this site it is reasonable to suggest that amplitude and phase analysis using waveform transformations, linear move-out and stacking, and common offset gathers are reasonably effective ways to locate and in some cases delineate subsurface anomalies such as pits, trenches, and buried utilities. It can also be stated with a reasonable

(a)

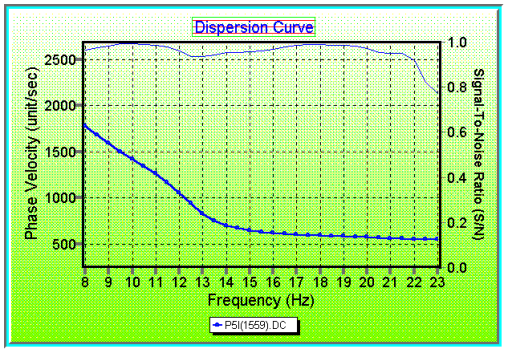

(b)

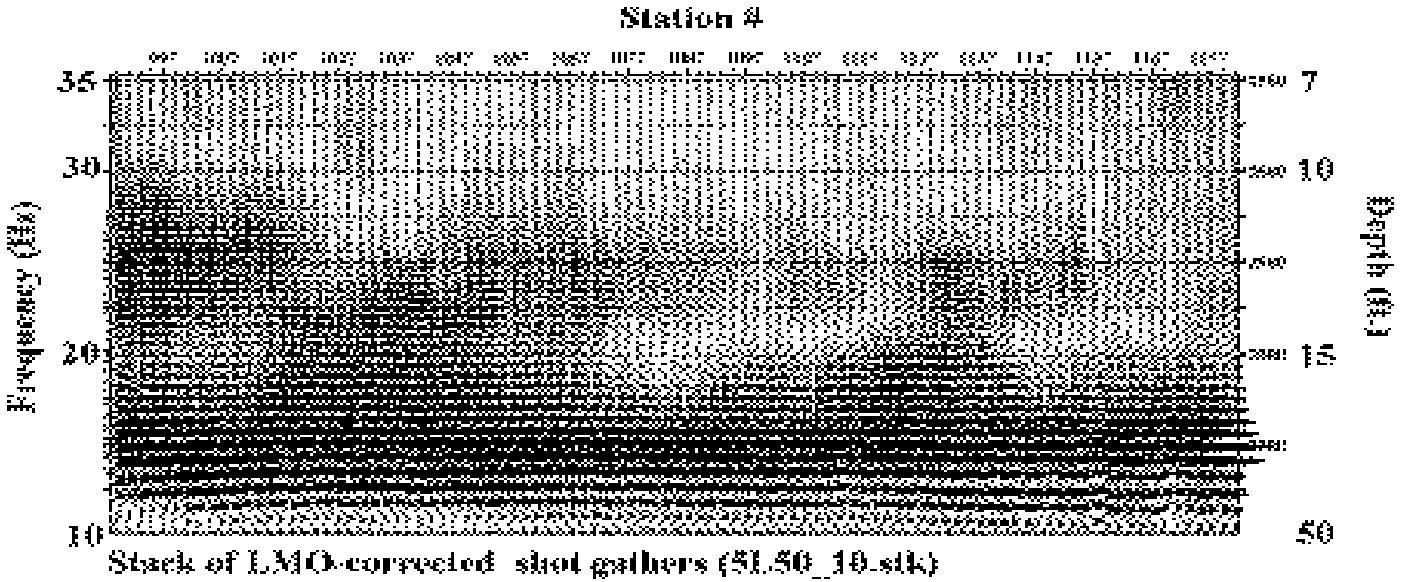

Figure 23. (a) A typical display of dispersion and S/N curves for line 5. (b) Wavefield transformation of shot gathers from line 5 similar to the section in Figure 4.

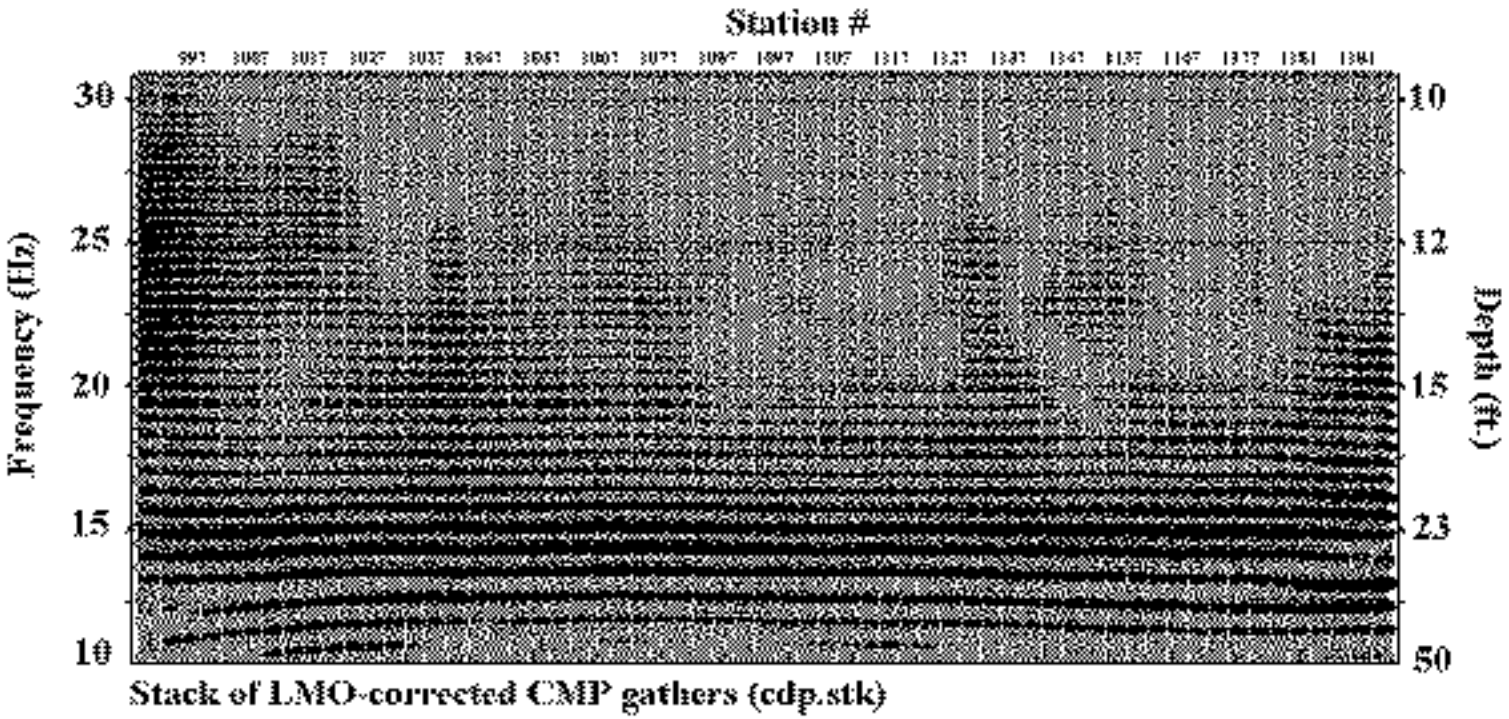

Figure 24. Wavefield transformation of CMP gathers from line 5.

(a)

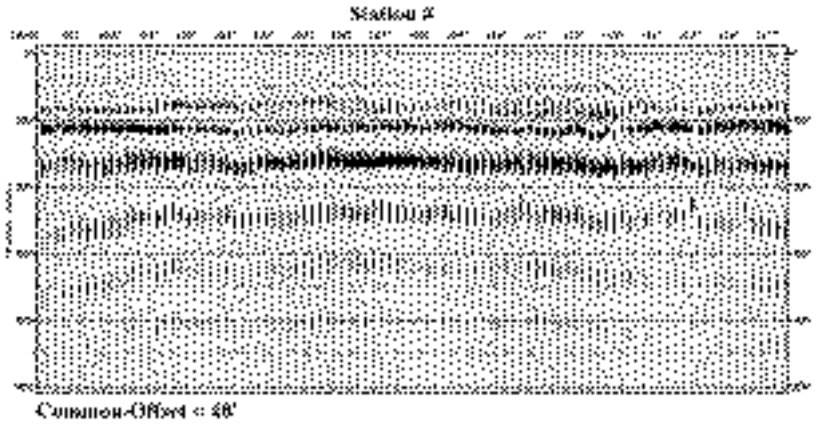

(b)

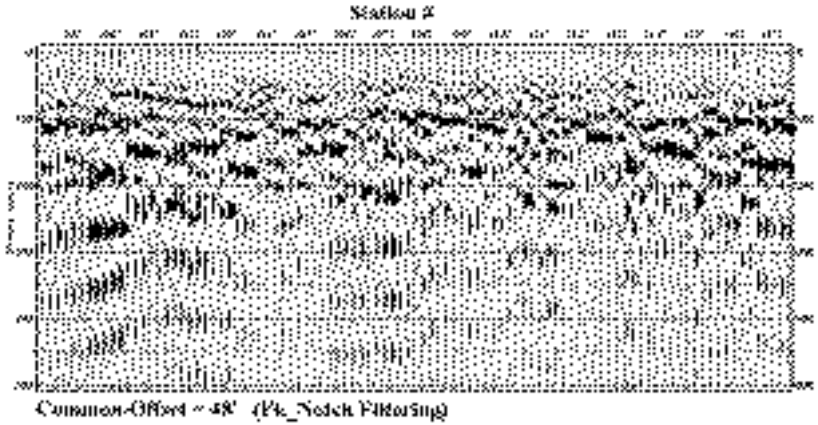

Figure 25. (a) Common-offset (48 ft) section of field records from line 5. (b) Section in (a) after F-K filter has been applied to filter out the horizontal event.

degree of confidence that the shear wave velocity field is quite useful at this site in delineating the base of compacted fill, boundaries between alluvial, glacial, and bedrock materials, and in some instances providing corroboration of anomalous features on waveform transformation that have been interpreted at depths generally greater than 5 ft and extending laterally more than half the spread length. Features, geologic contacts, and the local consistency in the velocity characteristics of these five sites needs to be evaluated with a well designed drilling program. At this point, correlating unique data characteristics with geologic features or engineering properties can only be accomplished with the aid of a program designed to provide ground truth.

Acknowledgments

Thanks to Randy Overton for the help and guidance during field work and while wading through the data processing and interpretations. Assistance in document preparation was provided by Mary Brohammer and Kyle Gregory.

References

Glover, R.H. 1959, Techniques used in interpreting seismic data in Kansas: in Symposium on Geophysics in Kansas, ed. W.H. Hambleton. Kansas Geological Survey Bulletin 137, p. 225-240.

Mayne, W.H., 1962, Horizontal data stacking techniques: Supplement to Geophysics, p. 927-937.

Miller, R.D., and J. Xia, 1999a, Using MASW to map bedrock in Olathe, Kansas: Kansas Geological Survey Open-file Report 99-9.

Miller, R.D., and J. Xia, 1999b, Seismic surveys at Alabama Electric Cooperative's proposed Damascus, Alabama site: Kansas Geological Survey Open-file Report 99-12.

Miller, R.D., J. Xia, and C.B. Park, 1999, MASW to investigate subsidence in the Tampa, Florida area: Kansas Geological Survey Open-file Report 99-33.

Nazarian, S., K.H. Stokoe II, and W.R. Hudson, 1983, Use of spectral analysis of surface waves method for determination of moduli and thicknesses of pavement systems, Transportation Research Record No. 930, 38-45.

Park, C.B., R.D. Miller, and J. Xia, 1996, Multi-channel analysis of surface waves using Vibroseis MASWV) [Exp. Abs.]: Soc. Expl. Geophys., p. 68-71.

Park, C.B., R.D. Miller, and J. Xia, 1997, Summary report on surface wave project at the Kansas Geological Survey: Kansas Geological Survey Open-file Report 97-80.

Park, C.B., R.D. Miller, and J. Xia, 1998, Ground roll as a tool to image near-surface anomaly [Exp. Abs.]: Soc. Explor. Geophys., p. 874-877.

Park, C.B., R.D. Miller, and J. Xia, 1999, Multi-channel analysis of surface waves: *Geophysics*, v. 64, n. 3, p. 800-808.

Steeples, D.W., and R.D. Miller, 1990, Seismic-reflection methods applied to engineering, environmental, and groundwater problems: Soc. Explor. Geophys. Investigations in Geophysics no. 5, S.H. Ward, ed., Vol. 1: Review and Tutorial, p. 1-30.

Xia, J., R.D. Miller, and C.B. Park, 1997, Estimation of shear wave velocity in a compressible Gibson half-space by inverting Rayleigh wave phase velocity: Technical Program with Biographies, SEG, 67th Annual Meeting, Dallas, TX, p. 1927-1920.

Xia, J., R.D. Miller, and C.B. Park, 1998, Construction of vertical seismic section of near-surface shear-wave velocity from groundroll [Exp. Abs.]: Soc. Explor. Geophys./AEGE/CPS, Beijing, p. 29-33.

Xia, J., R.D. Miller, and C.B. Park, 1999, Estimation of near-surface shear-wave velocity by inversion of Rayleigh wave: *Geophysics*, v. 64, p. 691-700.

Xia, J., R.D. Miller, C.B. Park, J.A. Hunter, and J.B. Harris, 2000, Comparing shear-wave velocity profiles from MASW technique with borehole measurements in unconsolidated sediments of the Fraser River Delta: *Journal of Environmental and Engineering Geophysics*.